isvr Institute of Sound and Vibration Research

Comparison of Ordinary Cross Validation and Generalized Cross Validation for Structure-borne Sound Source Identification

H.G. Choi, A.N. Thite and D.J. Thompson

ISVR Technical Memorandum 914

July 2003

University of Southampton

SCIENTIFIC PUBLICATIONS BY THE ISVR

Technical Reports are published to promote timely dissemination of research results by ISVR personnel. This medium permits more detailed presentation than is usually acceptable for scientific journals. Responsibility for both the content and any opinions expressed rests entirely with the author(s).

Technical Memoranda are produced to enable the early or preliminary release of information by ISVR personnel where such release is deemed to the appropriate. Information contained in these memoranda may be incomplete, or form part of a continuing programme; this should be borne in mind when using or quoting from these documents.

Contract Reports are produced to record the results of scientific work carried out for sponsors, under contract. The ISVR treats these reports as confidential to sponsors and does not make them available for general circulation. Individual sponsors may, however, authorize subsequent release of the material.

UNIVERSITY OF SOUTHAMPTON

INSTITUTE OF SOUND AND VIBRATION RESEARCH

DYNAMICS GROUP

Comparison of Ordinary Cross Validation and Generalized Cross Validation for Structure-borne Sound Source Identification

by

H.G. Choi, A.N. Thite and D.J. Thompson

ISVR Technical Memorandum No: 914

July 2003

Authorised for issue by
Professor M.J. Brennan
Group Chairman

LIST OF CONTENTS

ACKNOWLEDGEMENT

This research was supported by the Post-doctoral Fellowship Program of Korea Science and Engineering Foundation (KOSEF), Daejeon-City, Korea.

1. INTRODUCTION

In performing transfer path analysis of structure-borne sound transmission, the operational forces at the excitation points and/or at the connections within the structure-borne paths are required. These can be obtained by using inverse techniques using a measured frequency response function matrix and a set of operational responses [1–4]. However such methods are sensitive to the conditioning of the matrix that has to be inverted. Since the measurements of the operational responses and the frequency response functions include some errors that cannot be known, the reconstructed forces and responses may contain large errors.

To reduce the errors caused by the inversion of the accelerance matrix, the singular value rejection method has been used in previous research [2,4,5]. This method usually results in reduced errors for the reconstructed forces.

Verheij [2] used un-correlated point forces to describe large mechanical sources while compact sources were represented in terms of correlated sources. The singular value rejection method was introduced in this work in order to improve the conditioning of the matrix inversion. Smaller singular values were rejected if they were corrupted by noise. A threshold to reject singular values was established based on estimates of the accelerance measurement errors. The equivalent forces method was then applied to studying sound transmission paths [3] for a ship engine and gearbox. Janssens *et al.* [1] applied this method to flanking paths of a diesel engine on a ship, in particular the drive shaft and cooling water pipes.

However, rejecting the singular values less than some threshold means the loss of some information. A small change in the threshold can result in a singular value being accepted or rejected which may make a significant change to the results. To overcome this, the singular values can be weighted such as in Tikhonov regularization. This

approach has been introduced in acoustic source identification [5, 6] and more recently inverse force determination [7]. In Tikhonov regularization, it is important to choose an optimal regularization parameter. Thite [7] used ordinary cross validation (OCV) [8] for choosing an optimal value and developed an alternative called selective cross validation (SCV).

In this study, the technique of generalized cross validation for selecting the optimal Tikhonov regularization parameter is also considered. Generalized cross validation (GCV), which was introduced by Golub *et al.* [9], is a rotation-invariant version of ordinary cross validation. This method has been applied to acoustic source identification problems [6] but not yet to structural dynamics problems. The results of GCV are compared with those of OCV and SCV using simulations on a flat rectangular plate, as in [7]. The robustness of each of these methods is assessed for different noise levels.

Also, the range of the regularization parameters to be used in each method for selecting the optimal value is investigated. Because the singular values of the accelerance matrix differ at each frequency, a frequency-dependent range for the regularization parameters is needed to reduce the inverse force determination errors. The initial range of regularization parameters considered is a full range, but this is inefficient to use. Therefore the several ranges of regularization parameter are used to investigate the effects of fixing the lower and the upper limits of regularization parameters.

In addition, the effects of various parameters on the performance of the methods of OCV and GCV are investigated. Those parameters varied in this study are the shape of plates, the damping value, the force positions (the relationship among force positions themselves and the relationship between force and response forces) and the

noise levels included in measured FRF's and operational responses. Considering these factors, the performance of OCV and GCV is compared for the average errors in reconstructed forces and optimal regularization parameters selected.

2. METHODS FOR SELECTING THE TIKHONOV REGULARIZATION PARAMETER

2.1. Tikhonov regularization

It is supposed that a vector of operational responses $\hat{a}$ are measured at some positions, and that the matrix of frequency response functions $\hat{A}$ from a set of force positions to the response positions are also measured. The objective is to find a vector of forces $\tilde{F}$ such that $\hat{a} \cong \hat{A}\tilde{F}$.

The measured operational responses $\hat{a}$ and the measured frequency response functions $\hat{A}$ contain some errors that are unknown. Therefore if it is supposed that the fitted force $\tilde{F}$ can be obtained, a fitting error can be defined as

$$\tilde{e} = \hat{a} - \hat{A}\tilde{F}. \tag{1}$$

To minimise these fitting errors $\tilde{e}$, Tikhonov suggested a cost function given by

$$J = (\tilde{e}^H \tilde{e}) + \lambda(\tilde{F}^H \tilde{F}) \tag{2}$$

or

$$J = (\hat{a} - \hat{A}\tilde{F})^H (\hat{a} - \hat{A}\tilde{F}) + \lambda(\tilde{F}^H \tilde{F}) \tag{3}$$

where λ is a regularization parameter and H indicates Hermitian transpose. For this cost function to be minimised, the first derivative of J with respect to the force vector $\tilde{F}$ must be zero. After differentiating with respect to each of the real and imaginary parts, the optimal solution to minimise the error amplification in force reconstruction is given by [5, 6]

$$\tilde{F} = (\hat{A}^H \hat{A} + \lambda I)^{-1} \hat{A}^H \hat{a}. \tag{4}$$

Using the singular value decomposition of the accelerance matrix, $\hat{A} = USV^H$, in which S is a diagonal matrix of singular values and U and V are unitary matrices, equation (4) can be represented as follows

$$\tilde{F} = V(S^H S + \lambda I)^{-1} S^H U^H \hat{a}\,. \tag{5}$$

Thus the singular value s_i becomes $s_i/(s_i^2 + \lambda)$ in the regularized inverse.

Now the problem is how to select an appropriate regularization parameter for the optimal force vector. To do this, it is necessary to know the errors in the measurement but, as previously stated, the errors cannot be known. Consequently several kinds of mathematical concept that approximate the errors are used, for example, ordinary cross validation, selective cross validation, generalized cross validation, etc. In the next sections, these methods are presented.

2.2. Ordinary cross validation

Allen suggested the method of ordinary cross validation (OCV) [8]. This method is also referred to as the PRESS method ('Prediction sum of squares' of deviation). In this method, the force vector $\tilde{F}_k$ is determined by using equation (5) with the measured operational responses except one (the *k*th). The difference is calculated between the *k*th measured operational response $\hat{a}_k$ and this response reconstructed by using the force vector obtained from the responses except the *k*th one $\hat{A}_k \tilde{F}_k$ where $\hat{A}_k$ is a vector containing the *k*th column of $\hat{A}$. Hence the ordinary cross validation function is defined as

$$V_O(\lambda) = \frac{1}{m}\sum_{k=1}^{m}\left|\hat{a}_k - \hat{A}_k \tilde{F}_k\right|^2 \tag{6}$$

where m is the number of responses. Equation (6) can be rewritten in matrix form as [9]

$$V_O(\lambda) = \frac{1}{m}\left\|B(\lambda)(I - C(\lambda))\hat{a}\right\|^2 \tag{7}$$

where $\|\cdot\|$ indicates the Euclidean norm, $C(\lambda)=\hat{A}(\hat{A}^H\hat{A}+\lambda I)^{-1}\hat{A}^H$ and $B(\lambda)$ is the diagonal matrix whose entries are given by $1/(1-c_{kk}(\lambda))$, $c_{kk}(\lambda)$ being the *kk*th entry of $C(\lambda)$. The derivation of equation (7) is given in Appendix A.

For a series of values of the regularization parameter, the cross validation function $V_O(\lambda)$ is calculated and the value of λ that corresponds to the minimum of $V_O(\lambda)$ is identified as the optimal value of regularization parameter. Using the optimal value of λ, the optimal forces and responses can be reconstructed using the full matrix $\hat{A}$. This process is carried out for each frequency.

Instead of minimising the sum of validation errors to choose the regularization parameter, the minimal value (over *k*) of validation errors can be used as follows

$$V_S(\lambda)=\min_k\left|\hat{a}_k-\hat{A}_k\tilde{F}_k\right|^2 \tag{8}$$

or

$$V_S(\lambda)=\min_k\left|\left[B(\lambda)(I-C(\lambda))\hat{a}\right]_k\right|^2. \tag{9}$$

This method is a variant of the method of ordinary cross validation developed by Thite [7] that is called 'selective cross validation' (SCV). The minimum validation error may correspond to the minimum value of the condition numbers of the submatrices of $\hat{A}$ with one row omitted.

2.3. Generalized cross validation

This method was suggested by Golub *et al.* [9]. In the extreme case where the entries of the measured frequency response functions $\hat{A}$ are 0 except for the *jj*th entries ($j=1,2,\cdots,m$), the matrix $C(\lambda)$ in equation (7) is diagonal, and consequently

$$V_O(\lambda)=\frac{1}{m}\|\hat{a}\|^2=\frac{1}{m}\sum_{k=1}^{m}|\hat{a}_k|^2. \tag{10}$$

In other words the force determining a_k is found to be 0 when a_k is omitted from $\hat{A}$, and so the reconstructed $a_k = 0$. In this case, the ordinary cross validation function is independent of the choice of the regularization parameter so that the method of ordinary cross validation would not perform very well in near diagonal cases. Therefore Golub *et al.* suggested a modification to the method of ordinary cross validation, called generalized cross validation (GCV), which follows from the argument that any good choice of λ should be invariant under rotation of the measurement coordinate system. Generalized cross validation is thus a rotation-invariant form of ordinary cross validation. This method may be derived as follows.

First, a matrix W is defined as a unitary matrix that diagonalizes the circulant matrices (see Appendix B). The entries of this matrix are given by

$$W_{jk} = \frac{1}{\sqrt{m}} e^{2\pi i(jk/m)}, \quad j,k = 1,2,\cdots,m \tag{11}$$

where m is the number of response positions.

Multiplying a matrix by W has the effect of applying a discrete Fourier transform to this matrix. It will be used for resolving the diagonal problem of the measured frequency response functions.

Next, using the singular value decomposition of the measured frequency response function $\hat{A}$, equation (1) can be written as

$$\tilde{e} = \hat{a} - USV^H \tilde{F}. \tag{12}$$

If this is pre-multiplied by U^H, this gives

$$U^H \tilde{e} = U^H \hat{a} - SV^H \tilde{F}, \tag{13}$$

and then pre-multiplication of equation (13) by W gives

$$WU^H \tilde{e} = WU^H \hat{a} - WSV^H \tilde{F}. \tag{14}$$

The transformed model is represented as

$$\tilde{e}_t = \hat{a}_t - \hat{A}_t \tilde{F} \tag{15}$$

where $\hat{a}_t = WU^H \hat{a}$ is the vector of transformed measured operational responses, $\hat{A}_t = WSV^H$ the vector of transformed frequency response functions, and $\tilde{e}_t = WU^H \tilde{e}$ the vector of transformed fitted errors.

By applying ordinary cross validation to this transformed model (15), the generalized cross validation function can be defined as

$$V_G(\lambda) = \frac{(1/m)\left\|(I - C_t(\lambda))\hat{a}_t\right\|^2}{[(1/m)\mathrm{Tr}(I - C_t(\lambda))]^2} \tag{16}$$

where $C_t(\lambda) = \hat{A}_t(\hat{A}_t^H \hat{A}_t + \lambda I)^{-1} \hat{A}_t^H$ is a circulant matrix and thus constant along the diagonals. Since $C(\lambda)$ and $C_t(\lambda)$ have the same eigenvalues, equation (16) can be written as (see Appendix C)

$$V_G(\lambda) = \frac{(1/m)\left\|(I - C(\lambda))\hat{a}\right\|^2}{[(1/m)\mathrm{Tr}(I - C(\lambda))]^2}. \tag{17}$$

Furthermore, it can also be shown [9] that $V_G(\lambda)$ is a weighted version of the ordinary cross validation function $V_O(\lambda)$ so that

$$V_G(\lambda) = \frac{1}{m}\sum_{k=1}^{m}\left|\hat{a}_k - \hat{A}_k \tilde{F}_k\right|^2 w_k \tag{18}$$

where $w_k = \left[\dfrac{1 - c_{kk}}{1 - (1/m)\mathrm{Tr}C(\lambda)}\right]^2$.

Using selective cross validation instead of ordinary cross validation for deriving the generalized cross validation function, the validation function (16) can be modified as follows

$$V_G(\lambda) = \min_k \frac{\left|(I - C_t(\lambda))\hat{a}_t\right|_k^2}{[(1/m)\mathrm{Tr}(I - C_t(\lambda))]^2}. \tag{19}$$

3. USE OF GENERALIZED CROSS VALIDATION

3.1. Analysis object

To evaluate the effectiveness of the method of generalized cross validation, a series of numerical simulations have been carried out based on a simply supported rectangular plate.

The plate is taken to have dimensions 600 mm × 500 mm × 1.5 mm and its material is steel (Young's modulus: 2.07×10^{11} N/m^2, Poisson's ratio: 0.3, density: 7850 kg/m^3, and damping loss factor: 0.03). Four positions were selected for applying coherent point forces perpendicular to the plate, and five positions for measuring operational responses. The locations of the force and accelerance measurement positions are shown in Table 1. A receiver position is also considered, located at (0.15a, 0.45b). The forces have broad-band spectra with constant rms amplitudes in each 1/3 octave band as listed in the table.

Table 1. Non-dimensional positions of forces and responses.

Force positions and rms amplitude				Response positions		
No	x/a	y/b	Force [N]	No	x/a	y/b
1	0.62	0.41	19.0	1	0.55	0.40
2	0.41	0.43	10.0	2	0.80	0.20
3	0.51	0.63	27.0	3	0.90	0.80
4	0.31	0.72	6.0	4	0.60	0.50
				5	0.20	0.30

The frequency range used for the simulations is from 10 Hz to 3.6 kHz. The plate response is dominated by individual modes at low frequencies and by multiple overlapping modes at high frequencies.

In these simulations, arbitrary noise signals are needed to produce 'measured' signals because an analytical model of the flexural vibration of a thin rectangular plate would otherwise have an exact solution without any noise. The so-called measurement noise was added to the acceleration and force signals [7]. The noise levels added to obtain operational responses and frequency response functions can be quantified by the average signal to noise ratio (S/N) across all 1/3 octave bands and are classified as low, medium and high. These values for the three levels of noise used are shown in Table 2. (Note that the S/N ratio varies with frequency [7].)

The numbers of averages that have been used in estimating FRF's and operational responses are 50 and 25, respectively.

The condition numbers of the measured frequency response functions in the presence of different noise levels are shown in Figure 1 and the frequency averaged condition number is given in Table 3.

Table 2. Average signal to noise ratios in dB indicating the level of noise added to signals to obtain operational responses and frequency response functions.

		Noise levels		
		Low (High S/N)	Medium (Medium S/N)	High (Low S/N)
Operational response		50.0	13.5	2.6
FRF	Acceleration	49.0	27.3	11.3
	Force	60.0	40.0	32.0

Table 3. Average condition number associated with the accelerance matrix due to different levels of noises.

		Noise levels in operational responses		
		Low	Medium	High
Noise levels in FRF's	Low	46.8	46.8	46.8
	Medium	17.2	17.2	17.2
	High	12.2	12.2	12.2

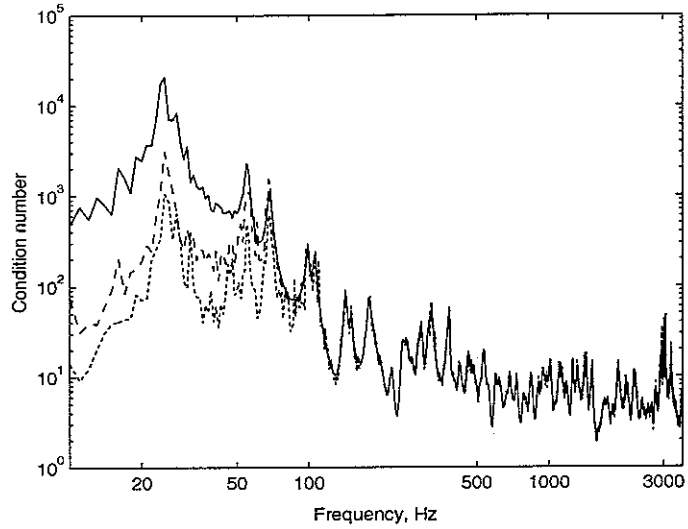

Figure 1. Condition numbers of the measured frequency response functions due to different levels of noise. —— low noise level, – – – medium, - - - - high.

3.2. Force determination and response reconstruction

Examples of the forces determined by using the various methods of cross validation are shown in Figure 2. OCV corresponds to minimising equation (7), SCV to equation (9), conventional GCV (GOCV) to equation (17) and GSCV to equation (19). The noise levels in the measurements correspond to low noise in the accelerances and medium noise in the responses. This case is chosen because in [7] it was found to be particularly difficult to obtain good results, especially at low frequency. All results are calculated in narrow bands and the results converted to 1/3 octave bands for presentation. Here, the true forces applied for all frequencies are shown in the right hand part of the figure. The forces are predicted more reliably at high frequencies than at low frequencies, and are better for the larger forces than the smaller ones. At low frequencies, large force determination errors result from high condition numbers.

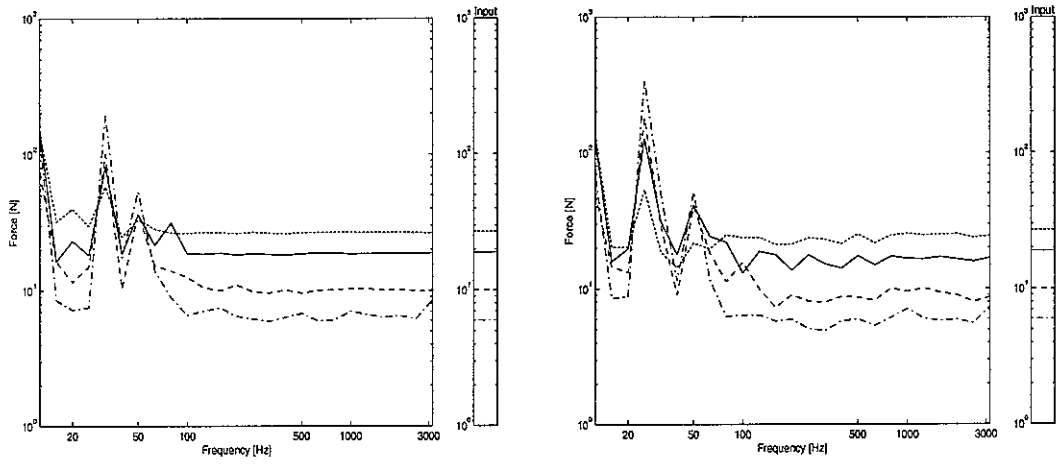

(a) OCV (b) SCV

(c) GOCV (d) GSCV

Figure 2. Reconstructed rms forces in 1/3 octave bands using low noise in accelerances and medium noise in the responses. —— force 1, – – – force 2, - - - - force 3, – · – · – force 4.

The reconstructed velocity response at the receiver location is shown in Figure 3, along with the true response at the same location. Except near 50 Hz, the reconstructed response is quite accurate, even though considerable errors exist in the forces determined at low frequencies. SCV and GSCV seem to give less reliable results at high frequencies than OCV and GOCV.

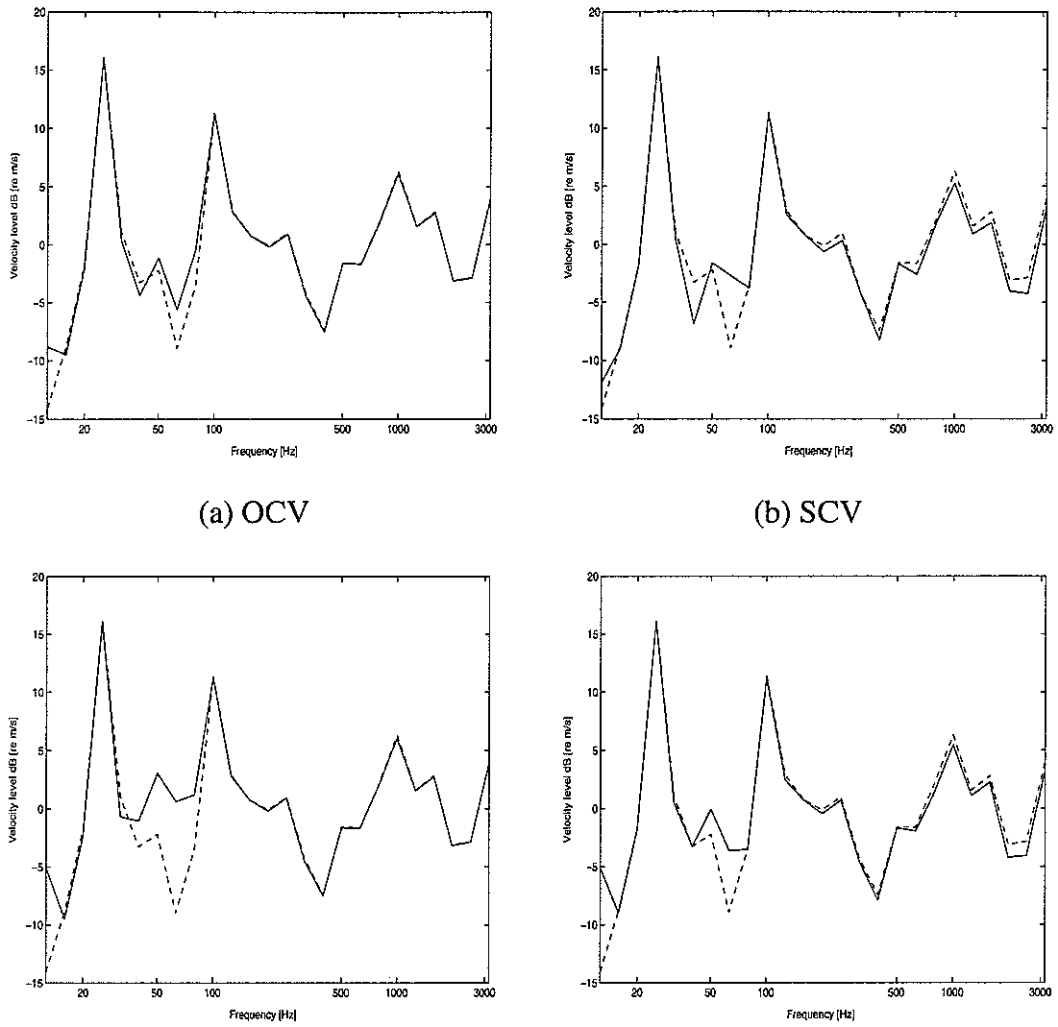

(a) OCV (b) SCV

(c) GOCV (d) GSCV

Figure 3. Reconstructed velocity response in 1/3 octave bands at the receiver location. – – – actual, —— reconstructed.

For the simulation considered, the forces and responses reconstructed using Tikhonov regularization with OCV are more reliable than with GCV, although GCV is equally good in the range above 100Hz.

3.3. Robustness for different noise levels

To investigate the robustness in selecting the regularization parameter for different levels of noise in responses and FRF's, calculations are performed for the various combinations of error identified in Table 3. Six methods are used to reconstruct forces

and the receiver response and their results are compared. These methods are as follows: ordinary cross validation, selective cross validation, generalized cross validation based on OCV and on SCV, minimum force error, and minimum response error. In the case of minimum force error, the fact that the forces are known is used to find the value of regularization parameter that minimises the force error. This represents an ideal case and shows the best that could be achieved. However it is not intended as a practical method. Similarly the minimum response error selects the regularization parameter on the basis of the calculated response at the receiver position without noise.

To select the regularization parameter for the global minimum value of the validation function at each frequency, the validation function is evaluated initially for a wide range of regularization parameters. This is determined as $\lambda = 0$, $s_{\max}^2 \times \{10^{-10}, \cdots, 1\}$ where $s_{\max}$ is the largest singular value and the parameters except 0 are logarithmically equally spaced values (50 points per decade).

Table 4 shows the average errors in the reconstructed forces and Table 5 shows the average errors in the reconstructed responses. The average error estimate used is given as follows

$$\varepsilon_{force} = \frac{1}{n}\sum_{j=1}^{n}\left[\frac{1}{N}\sum_{k=1}^{N}\left|L_{\tilde{F},j} - L_{F,j}\right|_k^2\right]^{1/2} \tag{20}$$

where ε_{force} is the average force error in dB, n is the number of force positions, N is the number of 1/3 octave bands k in the frequency range considered (here 25), $L_{\tilde{F},j}$ is the reconstructed jth force in 1/3 octave bands in dB and $L_{F,j}$ is the actual force in 1/3 octave bands in dB.

Table 4. Average errors in forces in dB calculated in 1/3 octave bands.

OCV		Noise levels in operational responses			SCV		Noise levels in operational responses		
		Low	Medium	High			Low	Medium	High
Noise levels in FRF's	Low	1.6	5.9	10.2	Noise levels in FRF's	Low	1.4	6.4	10.4
	Medium	1.6	3.3	5.5		Medium	2.2	3.1	6.7
	High	3.2	2.9	4.1		High	3.2	3.0	3.7
GOCV		Noise levels in operational responses			GSCV		Noise levels in operational responses		
		Low	Medium	High			Low	Medium	High
Noise levels in FRF's	Low	1.6	8.9	15.9	Noise levels in FRF's	Low	1.0	6.9	13.8
	Medium	1.6	4.0	7.8		Medium	1.8	3.3	5.9
	High	3.2	3.3	4.6		High	3.5	2.5	4.2
MFE		Noise levels in operational responses			MRE		Noise levels in operational responses		
		Low	Medium	High			Low	Medium	High
Noise levels in FRF's	Low	0.4	1.1	1.6	Noise levels in FRF's	Low	1.3	5.2	9.3
	Medium	1.0	1.3	1.8		Medium	1.9	3.3	5.2
	High	1.8	1.7	2.1		High	2.9	3.6	3.7

Table 5. Average errors in reconstructed response in dB calculated in 1/3 octave bands.

OCV		Noise levels in operational responses			SCV		Noise levels in operational responses		
		Low	Medium	High			Low	Medium	High
Noise levels in FRF's	Low	0.1	1.4	2.9	Noise levels in FRF's	Low	0.7	1.6	2.7
	Medium	0.3	0.9	3.6		Medium	1.5	1.3	3.8
	High	1.3	1.7	2.0		High	2.2	2.5	1.9
GOCV		Noise levels in operational responses			GSCV		Noise levels in operational responses		
		Low	Medium	High			Low	Medium	High
Noise levels in FRF's	Low	0.1	3.0	6.8	Noise levels in FRF's	Low	0.2	2.2	5.4
	Medium	0.4	2.4	4.7		Medium	0.8	2.0	4.0
	High	1.3	1.7	1.9		High	2.0	2.2	1.7
MFE		Noise levels in operational responses			MRE		Noise levels in operational responses		
		Low	Medium	High			Low	Medium	High
Noise levels in FRF's	Low	0.1	0.6	1.1	Noise levels in FRF's	Low	0.1	0.3	0.4
	Medium	0.3	0.8	1.1		Medium	0.2	0.3	0.4
	High	1.2	1.1	1.6		High	0.5	0.4	0.6

For the four methods of OCV, SCV, GOCV, and GSCV, the inverse force determination is observed to be very sensitive to the noise level in the response when the condition numbers are large (i.e. low FRF error). The forces determined by GCV

are a little worse than those by OCV because this system does not have any problem with near-diagonal matrices. The reconstructed responses (Table 5) contain smaller errors than the individual forces (Table 4). It is observed that OCV is more reliable than GCV for the responses as well. Selective cross validation does not give consistently better results than ordinary cross validation. In fact OCV is generally better in many cases.

However, comparing OCV with MFE, not surprisingly OCV is worse than MFE for both forces and responses. Apart from the difference in error levels between OCV and MFE, it is interesting to note that the average errors of forces obtained by MFE increase as the noise levels increase not only in FRF's but also in operational responses. By contrast the average errors of forces reconstructed by OCV are largest for high noise levels in the operational responses and low noise levels in the FRF's. Thus for medium and high noise levels in operational responses, the average errors of the forces by OCV decrease as the noise level in FRF's increases due to the effect of noise on the condition number (see Figure 1). The other methods show a similar trend to this.

Figure 4 shows the regularization parameters chosen to minimize the ordinary cross validation function for low/high noise levels in FRF's and low/high noise levels in operational responses. Also shown in each case are the maximum singular value squared, $s_{\max}^2$, 10^{-10} times this, the minimum singular value squared, $s_{\min}^2$, and the square of the error norm $\|E\|^2$ of the matrix $\hat{A}$. When zero values are selected for λ, these are shown along the bottom of the graph. It can be seen that the selected regularization parameters are shifted upward as the noise levels in FRF's and/or in operational responses become larger. It is observed that the selected regularization parameter generally increases as the frequency increases (in proportion to the square

of the largest singular value). It also increases as the condition number of the accelerance matrix decreases and as the noise level in operational response increases.

Figure 5 shows, for each method, the regularization parameters chosen to minimize the corresponding validation function. These results correspond to low noise in the FRF's and medium noise in the operational responses. In Figure 5, the trends of the results from the six methods are similar.

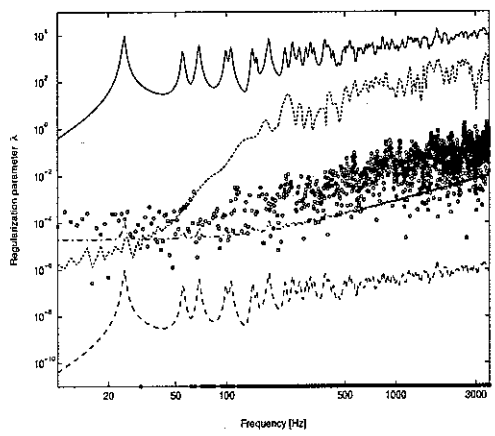

(a) low resp. noise – low FRF noise

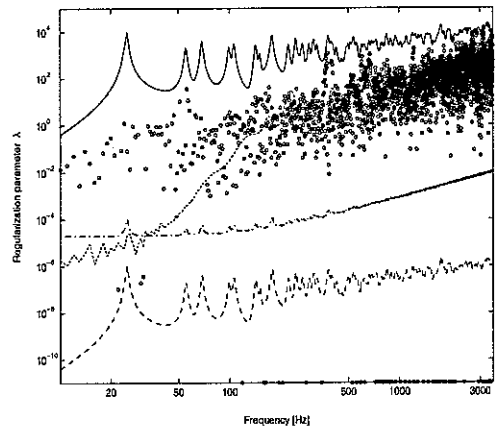

(b) high resp. noise – low FRF noise

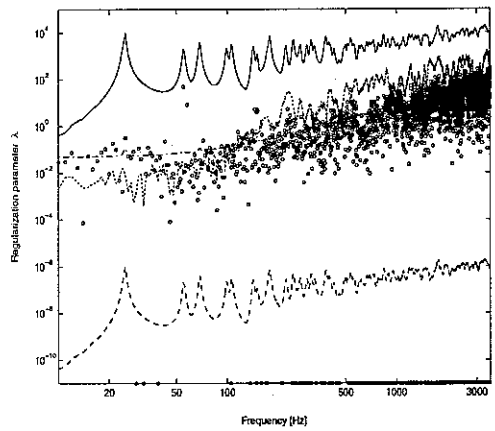

(c) low resp. noise – high FRF noise

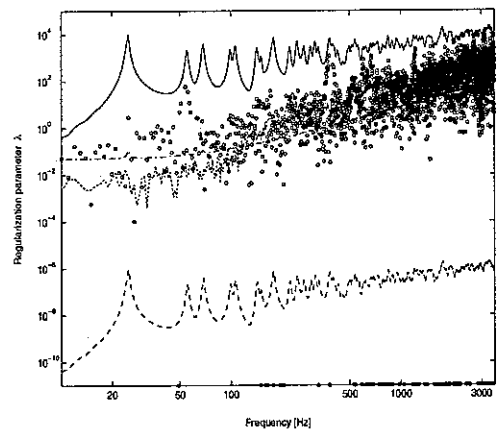

(d) high resp. noise – high FRF noise

Figure 4. Regularization parameters chosen by the method of ordinary cross validation for different noise levels (○).

—— $s_{\max}^2$, – – – $10^{-10} \cdot s_{\max}^2$, - - - - $s_{\min}^2$, – · – · – $\|E\|^2$.

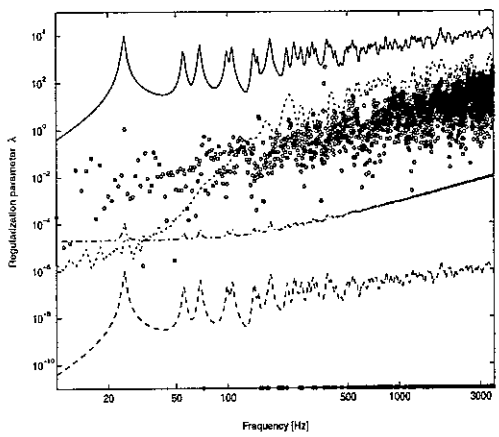

(a) OCV

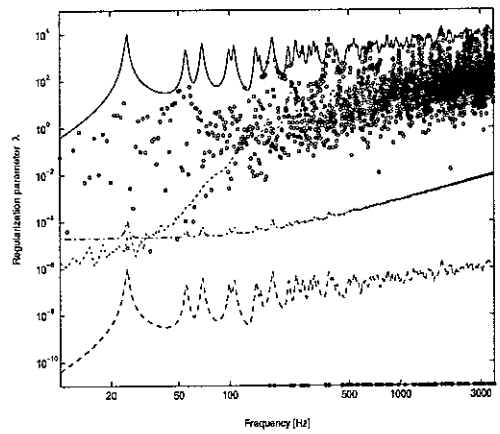

(b) SCV

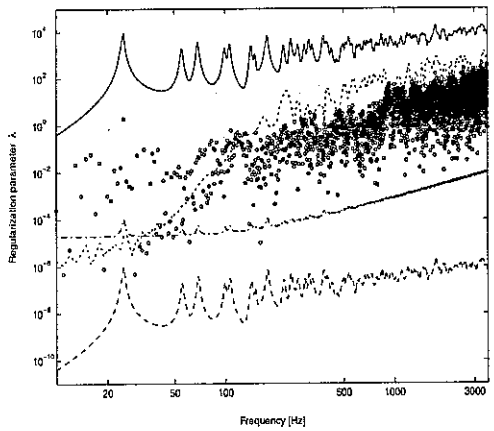

(c) GOCV

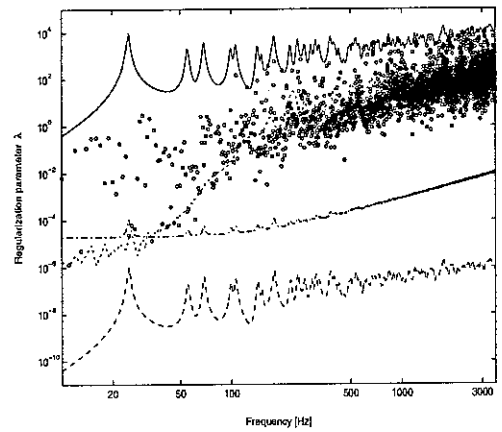

(d) GSCV

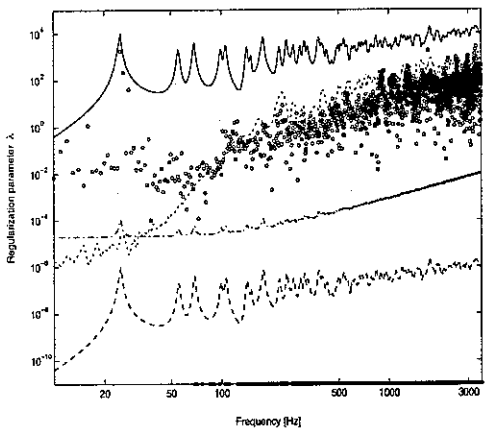

(e) MFE

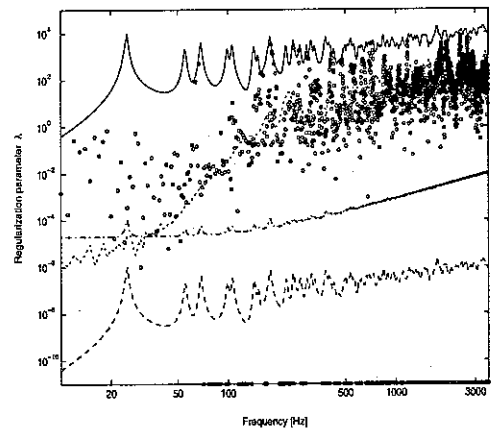

(f) MRE

Figure 5. Selected regularization parameters for low noise level in FRF's and medium noise level in operational responses (○).

—— $s_{\max}^2$, – – – $10^{-10} \cdot s_{\max}^2$, - - - - $s_{\min}^2$, – · – · – $\|E\|^2$.

Figure 6 shows the validation functions plotted against the regularization parameter for the different methods for specific frequencies, 25, 50, 100, and 400 Hz. The minima of the curves correspond to the optimal regularization parameters selected at each frequency. At low frequencies, the regularization parameters chosen by the different methods are spread out over the whole range considered, but the range of the selected regularization parameters becomes narrower at high frequencies. It is thought that the reason is the ill-conditioning of the accelerance matrix of low frequencies—the condition number has its maximum at 25 Hz which is the natural frequency of the first mode of the plate.

The SCV and GSCV methods produce validation functions that contain several local minima due to the effects of the different submatrices of $\hat{A}$. This may make them less reliable than the OCV and GOCV methods where a single global minimum is seen.

Figure 6 also shows the condition number of the regularized matrix as a function of regularization parameter. This generally has a minimum for a value of regularization parameter close to the optimal value, although it cannot be used as a reliable means of selecting λ as it takes no account of the operational responses and their noise levels.

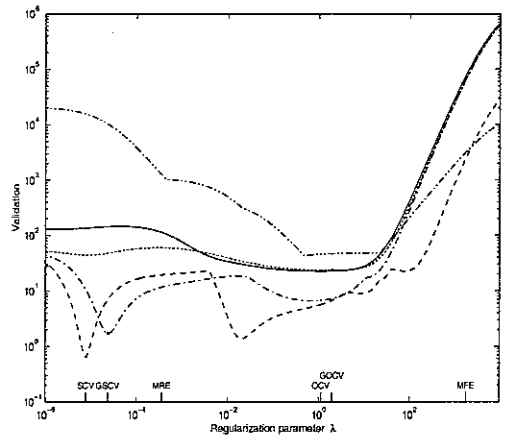

(a) 25 Hz

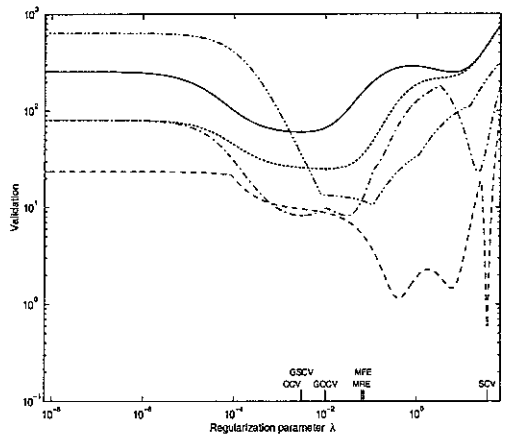

(b) 50 Hz

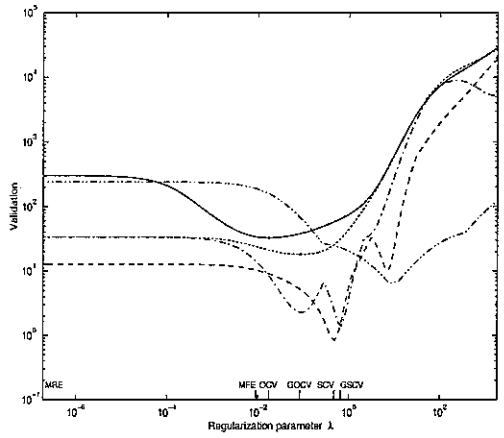

(c) 100 Hz

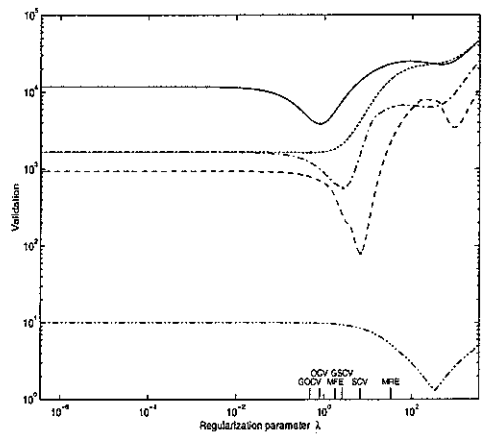

(d) 400 Hz

Figure 6. Validation functions against regularization parameter λ for the different methods for specific frequencies. —— OCV, – – – SCV, - - - - GOCV, – - – - – GSCV, – - – - – - – condition number.

4. GOOD INITIAL RANGE OF REGULARIZATION PARAMETERS

4.1. Introduction

In the previous section, the initial range of regularization parameters used to select the optimal regularization parameter was $\lambda = 0, s_{\max}^2 \times \{10^{-10}, \cdots, 1\}$. This range is wider than used by Thite [7] so it was found that his results sometimes used an inappropriate range. However this range is too wide to be efficient to use. Therefore the range needs to be optimised.

To find a more effective range of the regularization parameters, three ways of selecting the range are proposed as follows:

Range I: square of minimum singular value $s_{\min}^2$ to square of maximum singular value $s_{\max}^2$

Range II: square of the norm of error matrix $\|E\|^2$ to $s_{\max}^2$

Range III: minimum of $s_{\min}^2$ and $\|E\|^2$ to $s_{\max}^2$

The upper limit is the same as that of the previous section because the regularization parameters chosen by the ideal method of minimum force error were found to be below the curve of the maximum singular value squared in Figures 4 and 5. However the lower limit used previously appears to be too low to be efficient to use. Although $\lambda = 0$ is often selected in Figures 4 and 5, Figure 6 shows that adding a small regularization parameter has very little effect on the validation function and is to be preferred. Otherwise the selected regularization parameters generally are larger than the square of the error norm or the minimum singular value squared except in

cases of high noise levels in the FRF's. Therefore these two values are considered as the lower limit.

4.2. Range I: s^2_{min} to s^2_{max}

The average errors of the forces determined by using this range are shown in Table 6, and those of the reconstructed responses in Table 7. Comparing these results with those obtained previously by using the wider range, the average errors of the forces increase for the cases where they were small and decrease where they were large. Consequently the variations of the average errors are reduced and the robustness for different noise levels is improved. A similar trend is seen for the average errors of the reconstructed responses, which also have smaller variations and are more consistent for different noise levels.

Figure 7 shows the regularization parameters chosen by the method of ordinary cross validation for low/high noises in FRF's and low/high noises in operational responses. Figure 8 shows the selected regularization parameters from each method for the case of low noise in FRF's and medium noise in operational responses. It can be seen that above 100 Hz the lower limit is selected as the optimal parameter many times. This would appear to indicate that the lower limit based on s^2_{min} is too high.

Table 6. Average errors in dB calculated in 1/3 octave bands in forces reconstructed using $\lambda = \{s_{\min}^2, \cdots, s_{\max}^2\}$.

OCV		Noise levels in operational responses		
		Low	Medium	High
Noise levels in FRF's	Low	2.3	4.7	3.3
	Medium	2.5	3.1	4.8
	High	2.9	2.8	3.9

SCV		Noise levels in operational responses		
		Low	Medium	High
Noise levels in FRF's	Low	3.5	4.8	9.0
	Medium	3.5	3.5	5.3
	High	4.0	4.0	4.1

GOCV		Noise levels in operational responses		
		Low	Medium	High
Noise levels in FRF's	Low	2.5	7.9	7.5
	Medium	2.5	3.4	6.2
	High	3.2	3.0	3.9

GSCV		Noise levels in operational responses		
		Low	Medium	High
Noise levels in FRF's	Low	3.2	7.2	6.9
	Medium	3.3	3.6	5.7
	High	3.7	3.5	3.9

MFE		Noise levels in operational responses		
		Low	Medium	High
Noise levels in FRF's	Low	2.1	2.1	2.0
	Medium	2.4	2.2	2.2
	High	2.6	2.4	2.4

MRE		Noise levels in operational responses		
		Low	Medium	High
Noise levels in FRF's	Low	3.0	4.6	7.7
	Medium	3.2	3.5	4.1
	High	3.6	3.9	3.6

Table 7. Average errors in dB calculated in 1/3 octave bands in response reconstructed using $\lambda = \{s_{\min}^2, \cdots, s_{\max}^2\}$.

OCV		Noise levels in operational responses		
		Low	Medium	High
Noise levels in FRF's	Low	1.3	1.5	1.5
	Medium	1.3	1.1	2.8
	High	1.7	1.7	2.2

SCV		Noise levels in operational responses		
		Low	Medium	High
Noise levels in FRF's	Low	2.4	2.3	2.8
	Medium	2.2	2.0	2.9
	High	2.6	2.8	2.6

GOCV		Noise levels in operational responses		
		Low	Medium	High
Noise levels in FRF's	Low	1.3	2.4	3.7
	Medium	1.2	1.8	3.5
	High	1.5	1.7	1.7

GSCV		Noise levels in operational responses		
		Low	Medium	High
Noise levels in FRF's	Low	2.1	2.5	2.7
	Medium	2.0	1.9	3.0
	High	2.3	2.4	2.0

MFE		Noise levels in operational responses		
		Low	Medium	High
Noise levels in FRF's	Low	1.4	1.2	1.3
	Medium	1.4	1.3	1.3
	High	1.7	1.7	1.8

MRE		Noise levels in operational responses		
		Low	Medium	High
Noise levels in FRF's	Low	1.3	1.1	0.9
	Medium	1.3	1.1	0.9
	High	1.4	1.3	1.1

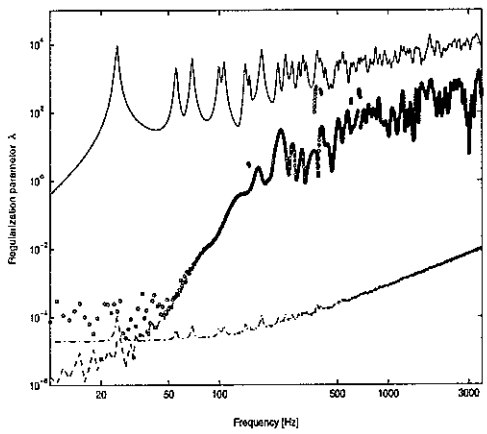

(a) low resp. noise – low FRF noise

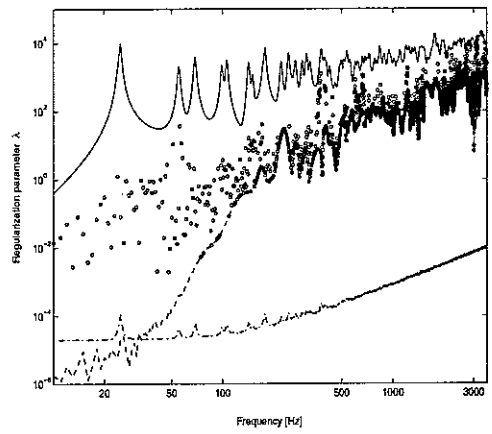

(b) high resp. noise – low FRF noise

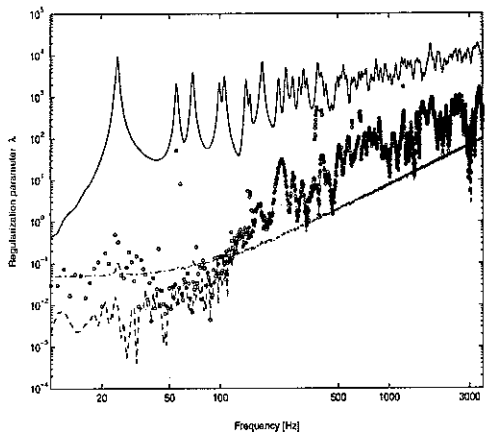

(c) low resp. noise – high FRF noise

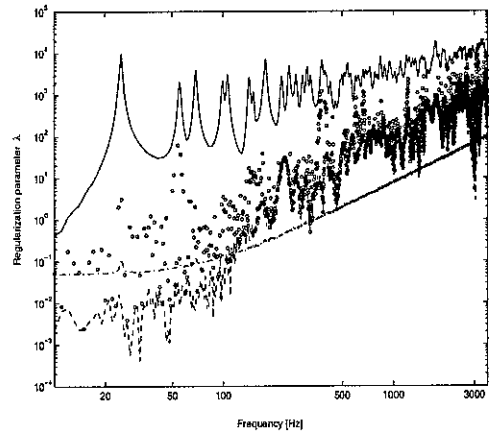

(d) high resp. noise – high FRF noise

Figure 7. Regularization parameters chosen from $\lambda = \{s_{\min}^2, \cdots, s_{\max}^2\}$ by the method of ordinary cross validation for different noise levels (○).

—— $s_{\max}^2$, – – – $s_{\min}^2$, – · – · – $\|E\|^2$.

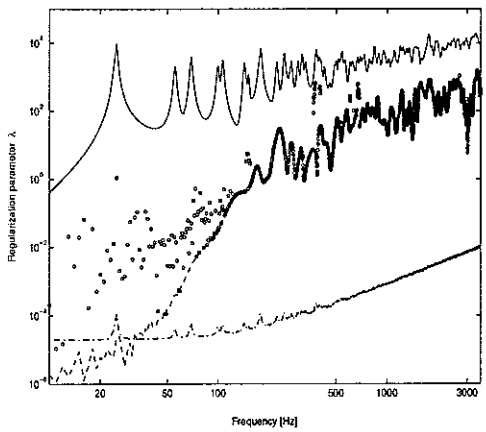

(a) OCV

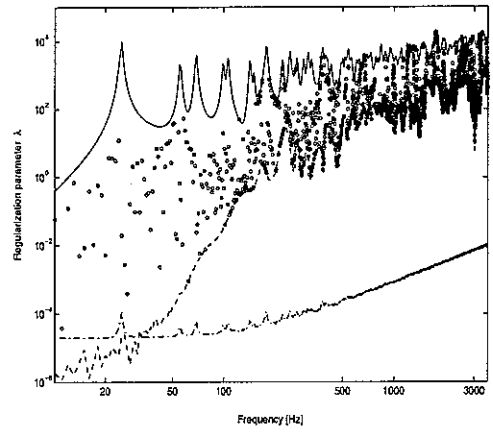

(b) SCV

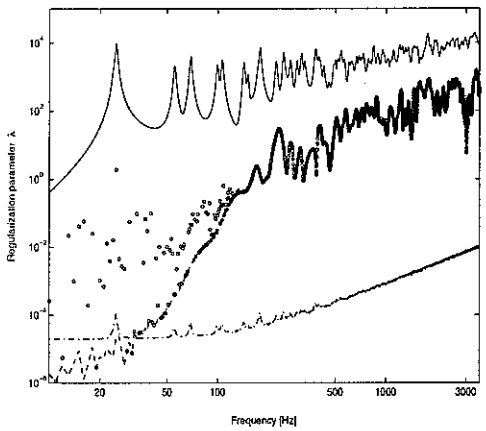

(c) GOCV

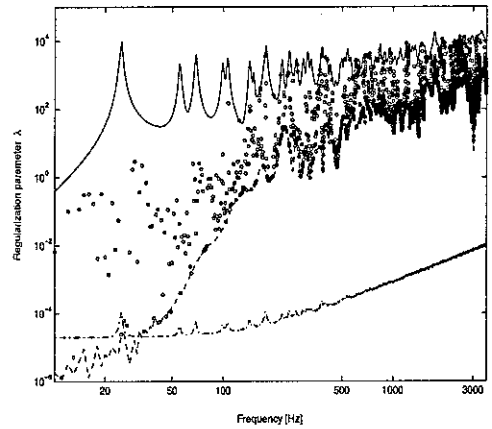

(d) GSCV

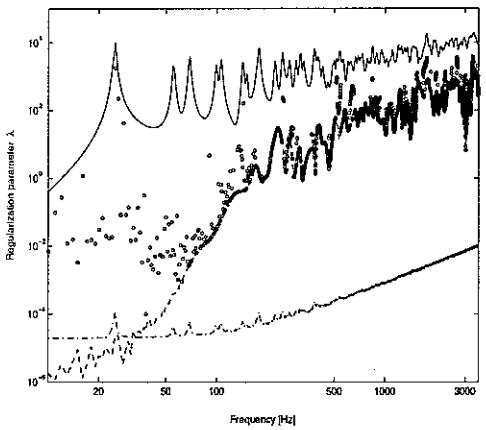

(e) MFE

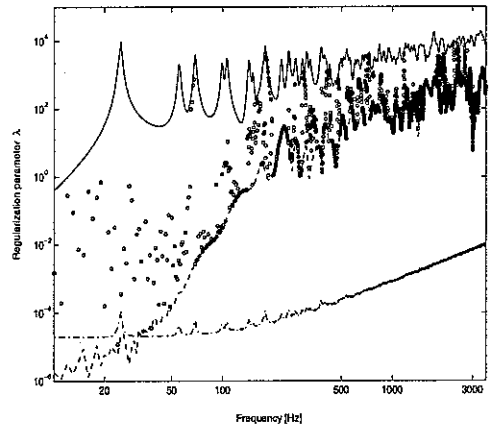

(f) MRE

Figure 8. Selected regularization parameters from $\lambda = \{s_{\min}^2, \cdots, s_{\max}^2\}$ for low noise level in FRF's and medium noise level in operational responses (○).

—— $s_{\max}^2$, – – – $s_{\min}^2$, –·–·– $\|E\|^2$.

4.3. Range II: $\|E\|^2$ to $s_{\max}^2$

The error norm is generally lower than the minimum singular value for the case with low FRF error (in fact in this study, the error norm is lower than the minimum singular value in the frequency range of $f > 30$ Hz for the case with low FRF error, $f > 70$ Hz for medium FRF error and $f > 100$ Hz for high FRF error). The average errors of the forces reconstructed by using the range based on $\|E\|^2$ are shown in Table 8, and those of the reconstructed responses in Table 9. Comparing the results from using range I with those from using range II, the force error is increased in only one case when using OCV or GOCV (high noise in operational responses and low noise in FRF's). Range II is thus seen to give improved results in the terms of the force determination error.

In the average errors of the reconstructed responses, the variation of errors is greater but the level of the maximum is similar. Thus here the range II also appears preferable.

Figure 9 shows the regularization parameters chosen by OCV for low/high noises in FRF's and low/high noises in operational responses. Figure 10 shows the selected regularization parameters for each method in the case of low noise in FRF's and medium noise in operational responses. The trend of the optimal regularization parameters is similar to that obtained from the full range, with the zero values replaced by $\|E\|^2$. Although the validation function is smaller for $\lambda = 0$ in these cases, the use of a small amount of regularization appears preferable in terms of the results in Tables 8 and 9.

Table 8. Average errors in dB calculated in 1/3 octave bands in forces reconstructed using $\lambda = \{\|E\|^2, \cdots, s_{\max}^2\}$.

OCV		Noise levels in operational responses			SCV		Noise levels in operational responses		
		Low	Medium	High			Low	Medium	High
Noise levels in FRF's	Low	0.6	4.4	3.6	Noise levels in FRF's	Low	1.4	4.4	8.4
	Medium	1.5	1.7	3.9		Medium	2.5	2.5	3.3
	High	2.6	2.6	3.2		High	3.7	3.8	3.6
GOCV		Noise levels in operational responses			GSCV		Noise levels in operational responses		
		Low	Medium	High			Low	Medium	High
Noise levels in FRF's	Low	0.5	6.4	9.6	Noise levels in FRF's	Low	0.9	4.8	5.8
	Medium	1.5	1.5	4.0		Medium	2.0	2.0	3.4
	High	2.6	2.5	3.1		High	3.2	2.9	3.6
MFE		Noise levels in operational responses			MRE		Noise levels in operational responses		
		Low	Medium	High			Low	Medium	High
Noise levels in FRF's	Low	0.3	1.1	1.6	Noise levels in FRF's	Low	1.3	4.6	7.4
	Medium	1.4	1.4	1.8		Medium	2.0	2.2	2.8
	High	2.5	2.3	2.3		High	3.0	3.0	3.2

Table 9. Average errors in dB calculated in 1/3 octave bands in response reconstructed using $\lambda = \{\|E\|^2, \cdots, s_{\max}^2\}$.

OCV		Noise levels in operational responses			SCV		Noise levels in operational responses		
		Low	Medium	High			Low	Medium	High
Noise levels in FRF's	Low	0.1	1.4	1.9	Noise levels in FRF's	Low	0.6	1.6	2.5
	Medium	0.7	0.4	1.5		Medium	1.6	1.3	2.1
	High	1.8	1.9	2.4		High	2.5	2.9	2.7
GOCV		Noise levels in operational responses			GSCV		Noise levels in operational responses		
		Low	Medium	High			Low	Medium	High
Noise levels in FRF's	Low	0.1	2.6	5.3	Noise levels in FRF's	Low	0.2	1.3	3.9
	Medium	0.7	0.4	2.0		Medium	1.2	0.7	1.8
	High	1.8	1.9	2.3		High	2.2	2.3	2.5
MFE		Noise levels in operational responses			MRE		Noise levels in operational responses		
		Low	Medium	High			Low	Medium	High
Noise levels in FRF's	Low	0.1	0.6	1.1	Noise levels in FRF's	Low	0.1	0.3	0.4
	Medium	0.7	0.7	1.0		Medium	0.6	0.4	0.4
	High	1.9	1.9	1.8		High	1.7	1.7	1.2

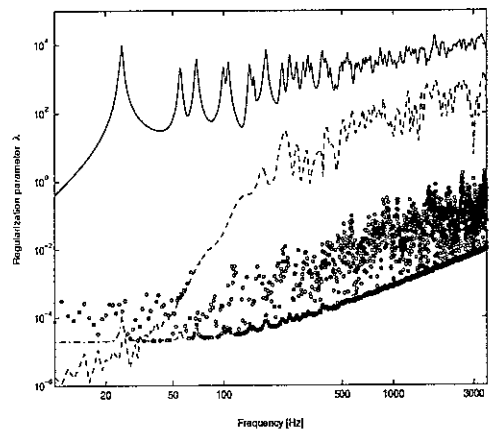

(a) low resp. noise – low FRF noise

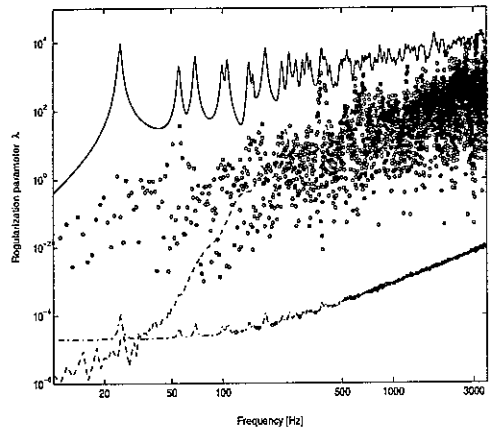

(b) high resp. noise – low FRF noise

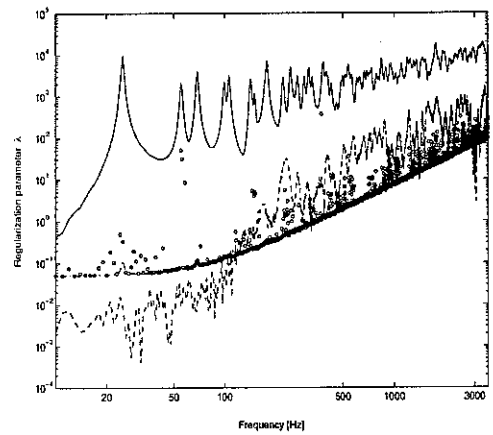

(c) low resp. noise – high FRF noise

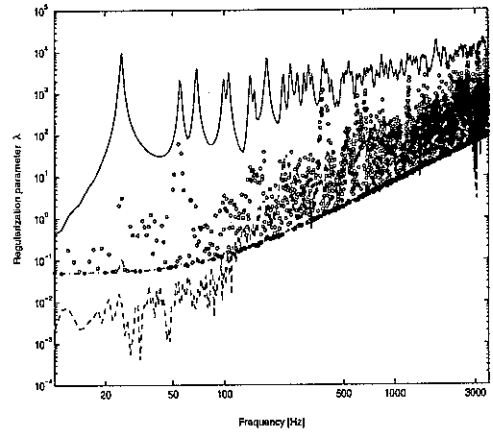

(d) high resp. noise – high FRF noise

Figure 9. Regularization parameters chosen from $\lambda = \{\|E\|^2_{\min}, \cdots, s^2_{\max}\}$ by the method of ordinary cross validation for different noise levels (○).

—— $s^2_{\max}$, – – – $s^2_{\min}$, – · – · – $\|E\|^2$.

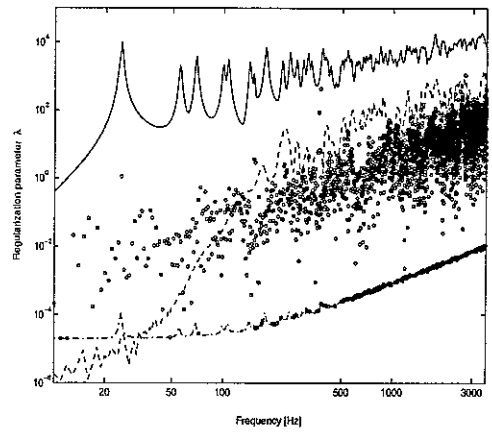

(a) OCV

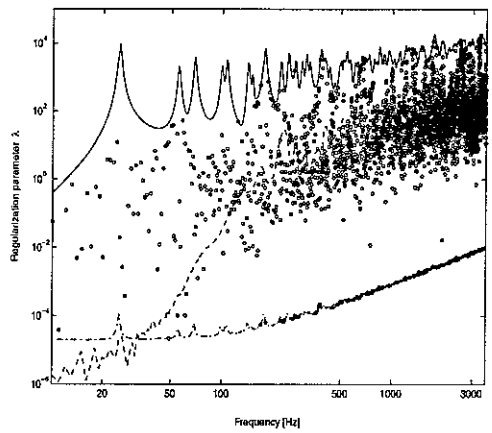

(b) SCV

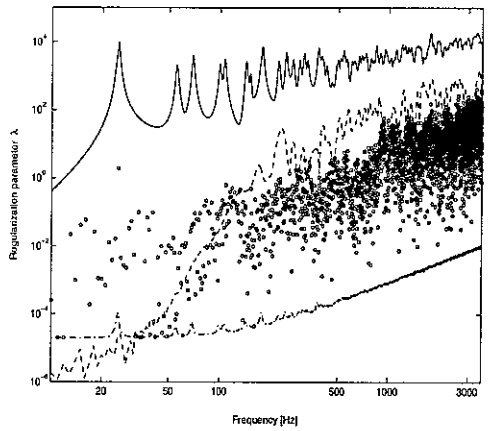

(c) GOCV

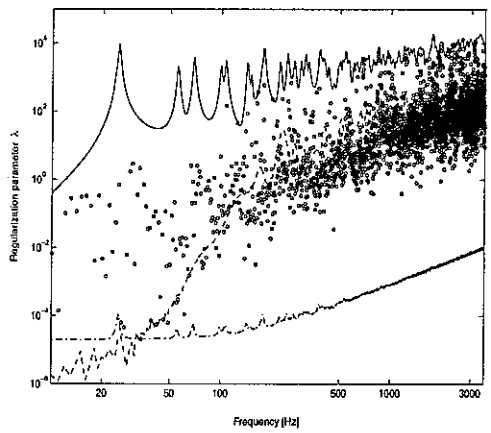

(d) GSCV

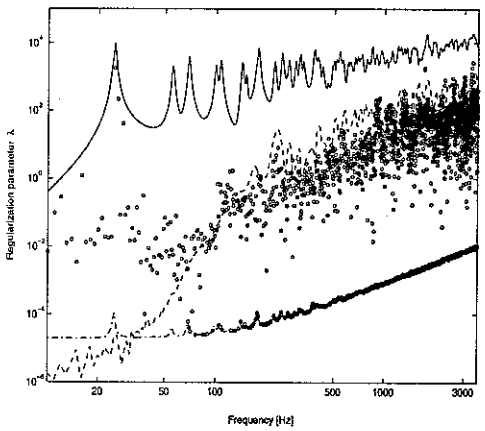

(e) MFE

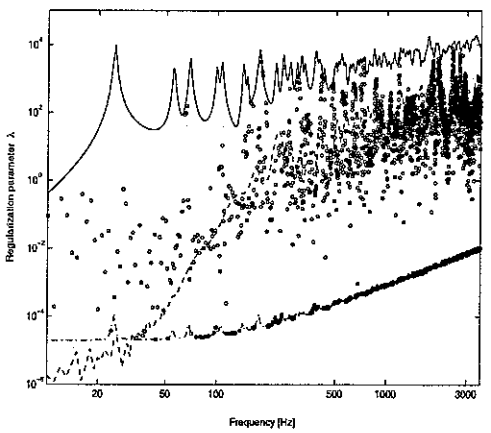

(f) MRE

Figure 10. Selected regularization parameters from $\lambda = \{\|E\|^2, \cdots, s_{\max}^2\}$ for low noise level in FRF's and medium noise level in operational responses (○).

—— $s_{\max}^2$, – – – $s_{\min}^2$, – · – · – $\|E\|^2$.

4.4. Range III: minimum of $s_{\min}^2$ and $\|E\|^2$ to $s_{\max}^2$

The average errors of the forces determined by using this range are shown in Table 10, and those of the reconstructed responses in Table 11. Compared with range II the average errors increase in some cases and decrease in other cases, but on the whole, range III is more reliable than range II. This conclusion is reached because the average errors of the forces obtained by the ideal method of minimum force errors decrease and the average errors of the responses obtained by the method of minimum response errors also decrease as the range used changes from range II to range III.

Figure 11 shows the regularization parameters chosen by the method of ordinary cross validation for low/high noise in FRF's and low/high noise in operational responses. The regularization parameters selected by the six methods in the case of low noise in FRF's and medium noise in operational responses are shown in Figure 12. The trend is similar to that of range II as in this case $s_{\min} < \|E\|$ only at low frequencies. In the case of high FRF error such as Figure 11 (c), the trend below 100 Hz is similar to that of range I, but the trend above 100 Hz is similar to that of range II.

It will be noted that OCV remains consistently better than GCV in most situations.

Table 10. Average errors in dB calculated in 1/3 octave bands in forces reconstructed using $\lambda = \{\min(s_{\min}^2, \|E\|^2), \cdots, s_{\max}^2\}$.

OCV		Noise levels in operational responses			SCV		Noise levels in operational responses		
		Low	Medium	High			Low	Medium	High
Noise levels in FRF's	Low	0.8	4.6	3.6	Noise levels in FRF's	Low	1.3	4.4	8.7
	Medium	1.5	2.4	4.9		Medium	2.3	2.5	4.8
	High	2.2	2.2	3.7		High	3.4	3.4	3.6
GOCV		Noise levels in operational responses			GSCV		Noise levels in operational responses		
		Low	Medium	High			Low	Medium	High
Noise levels in FRF's	Low	1.2	8.1	9.7	Noise levels in FRF's	Low	1.0	6.8	8.1
	Medium	1.5	2.9	6.3		Medium	2.0	2.4	5.5
	High	2.7	2.4	3.7		High	2.9	2.7	3.4
MFE		Noise levels in operational responses			MRE		Noise levels in operational responses		
		Low	Medium	High			Low	Medium	High
Noise levels in FRF's	Low	0.3	1.1	1.6	Noise levels in FRF's	Low	1.3	4.7	7.8
	Medium	1.2	1.3	1.8		Medium	1.9	2.5	3.7
	High	2.0	1.8	2.2		High	2.8	3.2	3.1

Table 11. Average errors in dB calculated in 1/3 octave bands in response reconstructed using $\lambda = \{\min(s_{\min}^2, \|E\|^2), \cdots, s_{\max}^2\}$.

OCV		Noise levels in operational responses			SCV		Noise levels in operational responses		
		Low	Medium	High			Low	Medium	High
Noise levels in FRF's	Low	0.1	1.4	1.9	Noise levels in FRF's	Low	0.6	1.6	2.5
	Medium	0.6	0.4	2.8		Medium	1.6	1.4	2.6
	High	1.4	1.5	2.1		High	2.2	2.4	2.3
GOCV		Noise levels in operational responses			GSCV		Noise levels in operational responses		
		Low	Medium	High			Low	Medium	High
Noise levels in FRF's	Low	0.1	2.9	5.3	Noise levels in FRF's	Low	0.2	2.2	3.9
	Medium	0.6	1.5	3.6		Medium	1.2	1.1	2.9
	High	1.2	1.4	1.6		High	1.9	2.0	1.6
MFE		Noise levels in operational responses			MRE		Noise levels in operational responses		
		Low	Medium	High			Low	Medium	High
Noise levels in FRF's	Low	0.1	0.6	1.1	Noise levels in FRF's	Low	0.1	0.3	0.4
	Medium	0.6	0.7	1.1		Medium	0.5	0.4	0.4
	High	1.3	1.3	1.7		High	1.0	0.8	0.7

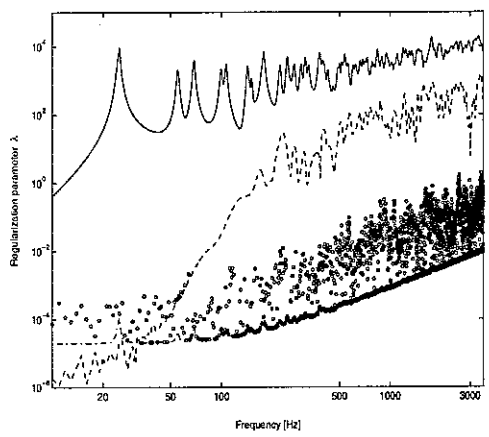

(a) low resp. noise – low FRF noise

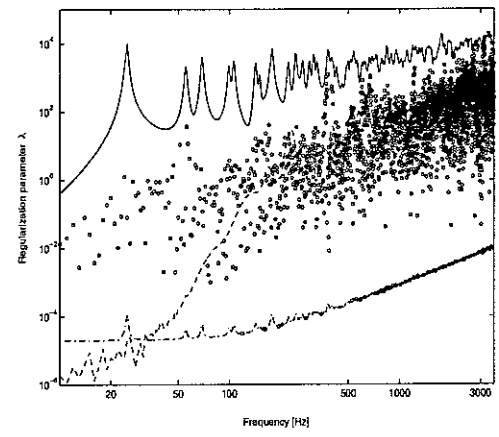

(b) high resp. noise – low FRF noise

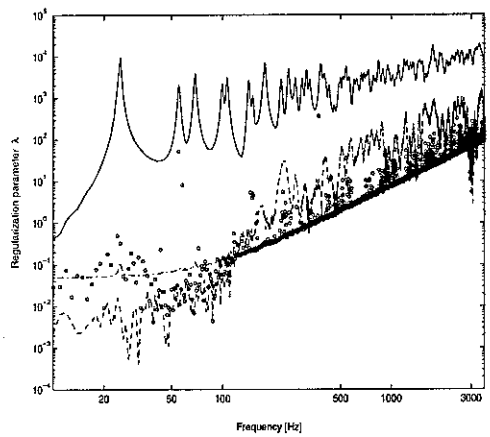

(c) low resp. noise – high FRF noise

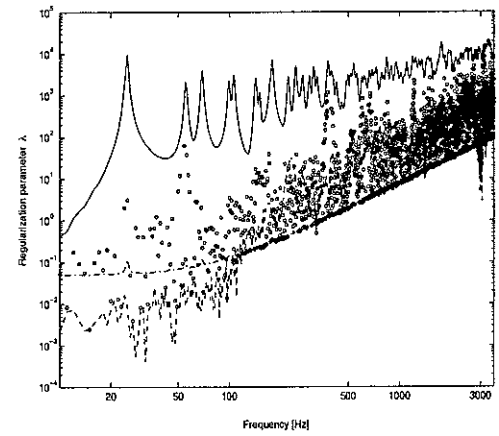

(d) high resp. noise – high FRF noise

Figure 11. Regularization parameters chosen from $\lambda = \{\min(s_{\min}^2, \|E\|^2), \cdots, s_{\max}^2\}$ by the method of ordinary cross validation for different noise levels (○).

—— $s_{\max}^2$, – – – $s_{\min}^2$, – · – · – $\|E\|^2$.

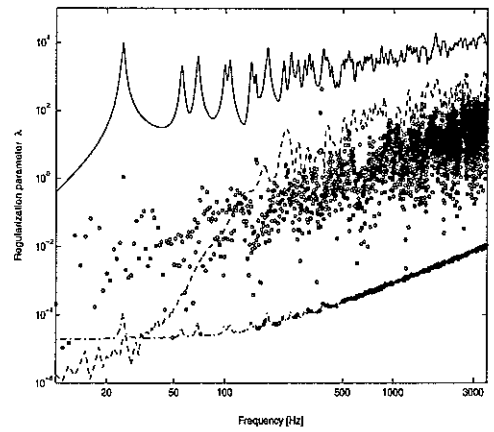

(a) OCV

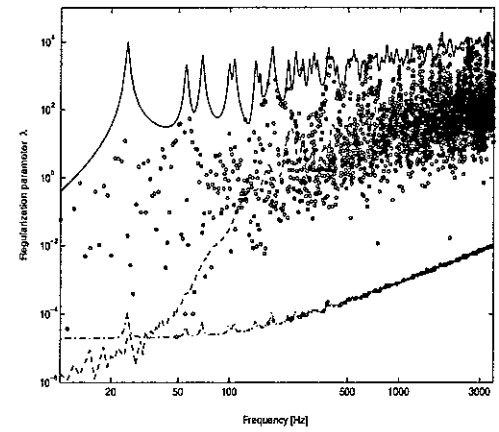

(b) SCV

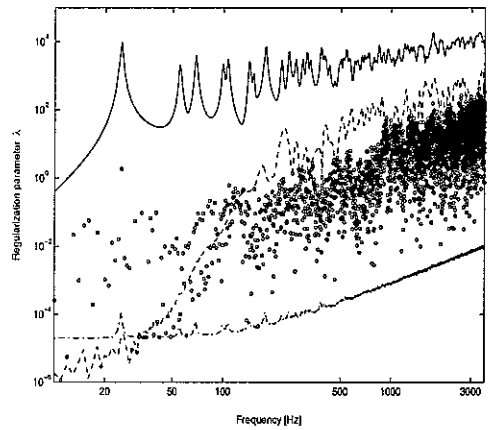

(c) GOCV

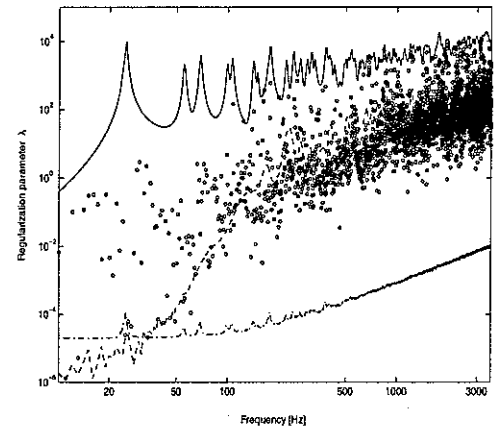

(d) GSCV

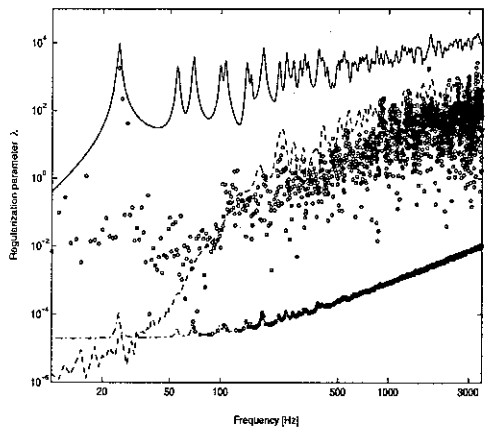

(e) MFE

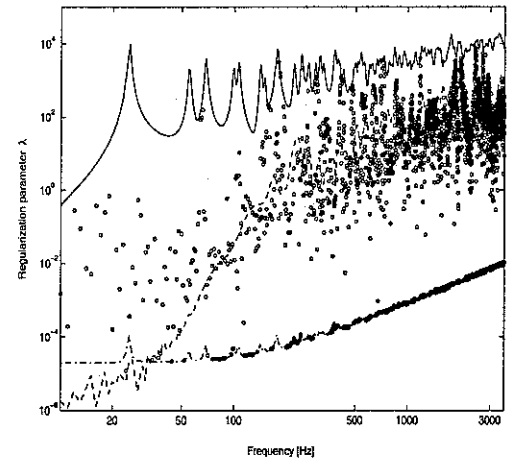

(f) MRE

Figure 12. Selected regularization parameters from $\lambda = \{\min(s_{\min}^2, \|E\|^2), \cdots, s_{\max}^2\}$ for low noise level in FRF's and medium noise level in operational responses (○).

—— $s_{\max}^2$, – – – $s_{\min}^2$, – · – · – $\|E\|^2$.

5. PERFORMANCE COMPARISON OF ORDINARY CROSS VALIDATION AND GENERALIZED CROSS VALIDATION

5.1. Introduction

In the previous section, the method of ordinary cross validation was found generally to show more reliable results than other Tikhonov regularization methods. However this conclusion is confined to the present condition, that is, the shape (the dimensions) and properties of the plate, the positions of the forces applied, and the noise added to the FRF's and the operational responses measured. Therefore, the effects of the variation of these parameters on the performance of the methods of OCV and GCV (hereafter GCV means GOCV for convenience) need to be investigated.

The parameters studied that are expected to have an effect on the performance of OCV and GCV, are the dimensions of the plate, the damping ratio, the position of the forces, and the signal-to-noise ratio in the FRF's and in the operational responses. In the case of the dimensions of the plate, the original plate (0.6×0.5 m), a square plate, and a strip each with same area were compared for the performance of the two methods. The other experimental conditions are the same as the original ones. Next, the damping ratio of the plate was varied to show the effect on the performance for the three values, i.e. the original, a smaller, and a larger value.

The distribution of force positions and moreover the relationship between the distributions of force and response positions are studied. Also the signal-to-noise ratio is of importance. This is considered separately in the next section.

Results are given first for the existing model. The existing plate has a dimension of 0.6 m $\times$ 0.5 m, a damping ratio of 3 %, and the positions of forces and responses are the same as those used in the previous chapters. However in this chapter, the frequency range used is from 10 Hz to 500 Hz because the results obtained by the two methods of OCV and GCV are similar to each other above 500 Hz. To estimate the

robustness of the methods for different noise levels, three noise levels in the operational responses and FRF's are used, which are the same as those used in the previous work. To compare the results exactly, the regularization parameters used to select the optimal one at each frequency are in the "full" range of 0 and 10^{-10} to 1 times the square of the maximum singular value at each frequency, as in section 3.

Table 12 shows the average errors in the reconstructed forces and Table 13 shows the average errors in the reconstructed responses. As seen in the tables, the average errors become larger than those obtained in the frequency range of 10 to 3600 Hz (see Tables 4 and 5) since the condition number in this case is generally larger than that in the previous case for the whole frequency range (see Figure 13).

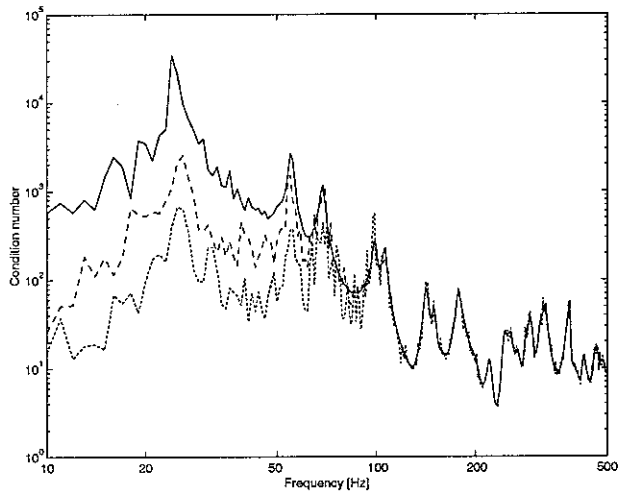

Figure 13. Condition numbers of the measured FRF's due to different levels of noise for the existing plate. —— low noise level, – – – medium, - - - - high.

Table 12. Average errors in dB calculated in 1/3 octave bands in forces reconstructed in the frequency range of 10 – 500 Hz for the existing plate.

OCV		Noise levels in operational responses			GCV		Noise levels in operational responses		
		Low	Medium	High			Low	Medium	High
Noise levels in FRF's	Low	1.8	9.6	13.4	Noise levels in FRF's	Low	1.6	10.5	17.3
	Medium	2.7	4.2	9.5		Medium	2.7	4.9	11.6
	High	2.6	3.3	4.7		High	2.7	3.4	6.4
MFE		Noise levels in operational responses			MRE		Noise levels in operational responses		
		Low	Medium	High			Low	Medium	High
Noise levels in FRF's	Low	0.4	1.4	2.2	Noise levels in FRF's	Low	2.0	9.0	10.3
	Medium	1.3	1.5	2.3		Medium	3.4	4.5	6.5
	High	2.0	2.0	2.4		High	2.8	3.3	5.6

Table 13. Average errors in dB calculated in 1/3 octave bands in responses reconstructed in the frequency range of 10 – 500 Hz for the existing plate.

OCV		Noise levels in operational responses			GCV		Noise levels in operational responses		
		Low	Medium	High			Low	Medium	High
Noise levels in FRF's	Low	0.2	1.2	6.4	Noise levels in FRF's	Low	0.1	1.2	8.6
	Medium	0.3	0.9	6.7		Medium	0.3	0.9	7.5
	High	1.0	0.9	2.4		High	1.1	1.4	4.6
MFE		Noise levels in operational responses			MRE		Noise levels in operational responses		
		Low	Medium	High			Low	Medium	High
Noise levels in FRF's	Low	0.1	0.5	1.5	Noise levels in FRF's	Low	0.1	0.2	0.4
	Medium	0.6	0.6	1.6		Medium	0.4	0.3	0.4
	High	0.9	0.9	1.6		High	0.6	0.5	0.6

5.2. Performance due to the variation of the dimensions of the plate

To study the effect of plate shape, three plates are considered: a rectangle with an aspect ratio of 6:5 (as before), a square, and a strip with an aspect ratio of 100:511. All three have the same area so the corresponding dimensions are 0.6 m × 0.5 m, 0.548 m × 0.548 m, and 0.242 m × 1.238 m, respectively. The non-dimensional positions of forces and responses are the same as those for the existing rectangular plate (Table 1). All other parameters and conditions, apart from the width and length of the plates, are not varied.

5.2.1. Square plate

Tables 14 and 15 show the average errors in reconstructed forces and responses, respectively for the square plate. The condition numbers are shown in Figure 14.

In comparison with the results of the rectangular plate, the average errors in forces reconstructed by OCV and GCV generally reduce by about 1 – 4 dB, except in the case of high noise level in FRF's, because the condition numbers become smaller in the case of low/medium noise levels in FRF's. The average errors in responses reconstructed by OCV and GCV become smaller especially in the case of high noise level in operational responses. Therefore since the differences of the average errors between by OCV and by GCV decrease, especially in the case of high noise level in operational responses, OCV and GCV show similar results. Nevertheless OCV mostly gives better results than GCV.

5.2.2. Strip plate

Tables 16 and 17 show the average errors in reconstructed forces and responses, respectively for the strip plate. Figure 15 shows the condition numbers.

After comparing the three plates, the average errors of forces for the strip plate are smaller than those for the other plates. This is because the condition numbers reduce considerably. However the differences between the errors in the forces obtained by OCV and by GCV are larger than those for the other plates in the cases of medium/ high noise levels in operational responses and low/medium noise levels in FRF's. Therefore in the case of the strip plates, OCV is generally superior to GCV.

The strip plate has different effects from other plates due to the large aspect ratio. This plate has a higher first natural frequency than the others but subsequent modes occur close together in frequency, and its mode shapes are essentially one dimensional below 250 Hz. These have effects on reducing the condition numbers and making OCV better than GCV.

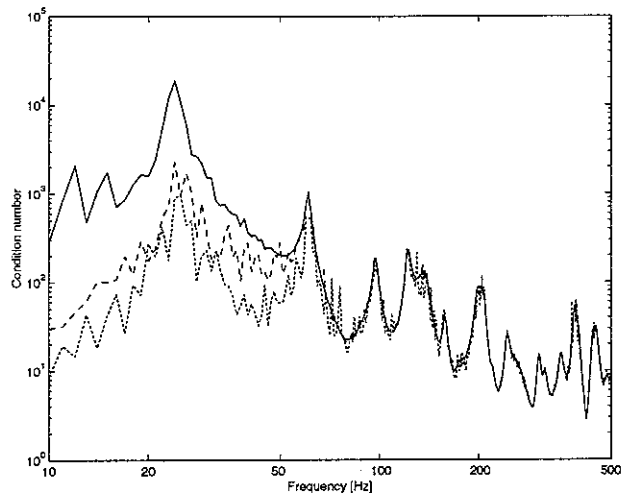

Figure 14. Condition numbers of the measured FRF's due to different levels of noise for the square plate. —— low noise level, – – – medium, - - - - high.

Table 14. Average errors in dB calculated in 1/3 octave bands in forces reconstructed in the frequency range of 10 – 500 Hz for the square plate.

OCV		Noise levels in operational responses			GCV		Noise levels in operational responses		
		Low	Medium	High			Low	Medium	High
Noise levels in FRF's	Low	1.0	5.1	12.8	Noise levels in FRF's	Low	1.2	6.2	14.3
	Medium	1.7	4.0	6.1		Medium	2.7	4.7	7.8
	High	3.4	3.3	4.5		High	3.4	3.9	5.2
MFE		Noise levels in operational responses			MRE		Noise levels in operational responses		
		Low	Medium	High			Low	Medium	High
Noise levels in FRF's	Low	0.3	1.3	2.0	Noise levels in FRF's	Low	1.4	6.4	14.3
	Medium	1.1	1.6	2.2		Medium	2.0	2.6	5.9
	High	2.1	2.0	2.4		High	3.0	3.5	4.3

Table 15. Average errors in dB calculated in 1/3 octave bands in responses reconstructed in the frequency range of 10 – 500 Hz for the square plate.

OCV		Noise levels in operational responses			GCV		Noise levels in operational responses		
		Low	Medium	High			Low	Medium	High
Noise levels in FRF's	Low	0.1	0.8	3.6	Noise levels in FRF's	Low	0.1	0.9	4.0
	Medium	0.4	0.3	1.8		Medium	0.4	0.5	2.3
	High	1.0	0.8	1.3		High	1.0	0.9	2.8
MFE		Noise levels in operational responses			MRE		Noise levels in operational responses		
		Low	Medium	High			Low	Medium	High
Noise levels in FRF's	Low	0.1	0.5	1.1	Noise levels in FRF's	Low	0.1	0.2	0.3
	Medium	0.3	0.6	1.2		Medium	0.2	0.2	0.3
	High	1.3	1.2	1.3		High	0.8	0.5	0.4

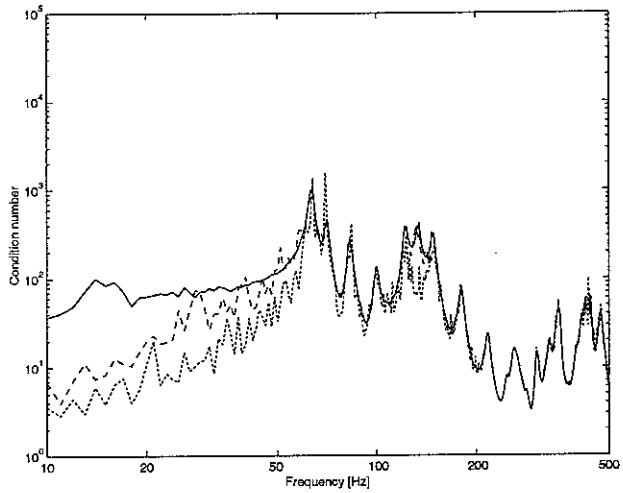

Figure 15. Condition numbers of the measured FRF's due to different levels of noise for the strip plate. —— low noise level, – – – medium, - - - - high.

Table 16. Average errors in dB calculated in 1/3 octave bands in forces reconstructed in the frequency range of 10 – 500 Hz for the strip plate.

OCV		Noise levels in operational responses			GCV		Noise levels in operational responses		
		Low	Medium	High			Low	Medium	High
Noise levels in FRF's	Low	0.8	3.5	10.3	Noise levels in FRF's	Low	0.8	8.9	12.9
	Medium	1.7	2.8	4.9		Medium	1.5	4.5	10.4
	High	2.4	3.2	4.5		High	2.4	3.4	5.7
MFE		Noise levels in operational responses			MRE		Noise levels in operational responses		
		Low	Medium	High			Low	Medium	High
Noise levels in FRF's	Low	0.3	1.5	1.8	Noise levels in FRF's	Low	0.8	5.1	8.9
	Medium	0.8	1.3	1.9		Medium	1.5	3.6	7.4
	High	1.5	1.7	2.0		High	2.4	3.1	5.4

Table 17. Average errors in dB calculated in 1/3 octave bands in responses reconstructed in the frequency range of 10 – 500 Hz for the strip plate.

OCV		Noise levels in operational responses			GCV		Noise levels in operational responses		
		Low	Medium	High			Low	Medium	High
Noise levels in FRF's	Low	0.4	0.9	2.5	Noise levels in FRF's	Low	0.4	3.3	5.0
	Medium	0.3	1.0	0.6		Medium	0.3	1.4	2.5
	High	1.7	2.3	2.6		High	1.7	2.4	2.9
MFE		Noise levels in operational responses			MRE		Noise levels in operational responses		
		Low	Medium	High			Low	Medium	High
Noise levels in FRF's	Low	0.5	0.7	0.9	Noise levels in FRF's	Low	0.1	0.2	0.5
	Medium	0.3	1.0	1.0		Medium	0.1	0.3	0.7
	High	0.8	1.8	1.9		High	0.6	1.0	0.4

5.3. Performance due to the variation of the damping ratio of the plate

Since the damping property affects the vibrational behaviour of the system its variation may have an effect on the performance of the methods of OCV and GCV. The existing damping ratio is 3 %. A smaller damping ratio of 1 % and a larger damping ratio of 10 % are considered here.

5.3.1. Small damping ratio

Tables 18 and 19 show the average errors in 1/3 octave bands in reconstructed forces and responses, respectively for the smaller damping ratio. The condition numbers are shown in Figure 16. These are generally higher at the resonances than for 3 % (see Figure 13).

From the tables it can be seen that as the damping ratio decreases the performances of OCV and GCV improve or remain similar to the previous ones except for the case of medium noise level in operational responses and low noise level in FRF's in spite of the increase of the condition numbers. This is because the reduction of the amplitude variation of the signals due to the decrease of the damping ratio is more effective on the performance of OCV and GCV than the increase of the condition numbers due to the same reason. Also, in comparison with each other, the performance of OCV is generally better than GCV and especially much better in the case of high noise level in operational responses with low noise level in FRF's.

5.3.2. Large damping ratio

Table 20 shows the average errors in reconstructed forces and Table 21 shows the average errors in reconstructed responses. The corresponding condition number plot is given in Figure 17.

Comparing these results with the two previous ones, the increased damping factor has positive and negative effects on the performances of OCV and GCV. The performance of OCV improves for high condition numbers with medium/high noise levels in the responses. The performance of GCV is better than for 1 % and 3 % for high noise levels in the responses.

Comparing the three results (initial, smaller and larger damping), both low and high damping ratios show better results than the initial value in some noise conditions and worse in others. As mentioned above, the low damping reduces the amplitude variation of the original signals and this is more effective on the performance of OCV and GCV than the added noise to the signals. In the case of the high damping, at high frequencies the condition numbers are lower at the resonances and the curves of the condition numbers are smooth. At low frequencies the condition numbers are similar to those for initial and smaller damping values. These different effects on the condition numbers with respect to the frequency range may have a positive effect in some cases and a negative effect in others.

However, the performance of OCV remains better than that of GCV in each case.

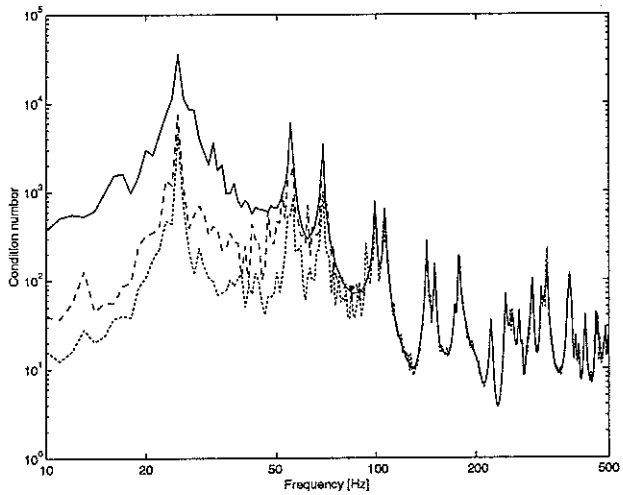

Figure 16. Condition numbers of the measured FRF's due to different levels of noise for the small damping ratio. —— low noise level, – – – medium, - - - - high.

Table 18. Average errors in dB calculated in 1/3 octave bands in forces reconstructed in the frequency range of 10 – 500 Hz for the small damping ratio.

OCV		Noise levels in operational responses			GCV		Noise levels in operational responses		
		Low	Medium	High			Low	Medium	High
Noise levels in FRF's	Low	1.2	12.2	8.7	Noise levels in FRF's	Low	1.5	13.5	16.3
	Medium	2.1	4.2	8.0		Medium	2.1	5.6	9.2
	High	2.9	2.7	4.0		High	2.8	3.1	4.4
MFE		Noise levels in operational responses			MRE		Noise levels in operational responses		
		Low	Medium	High			Low	Medium	High
Noise levels in FRF's	Low	0.4	1.5	2.0	Noise levels in FRF's	Low	1.9	9.9	8.3
	Medium	1.2	1.7	2.2		Medium	2.3	3.8	6.5
	High	1.8	1.9	2.5		High	2.7	3.0	5.2

Table 19. Average errors in dB calculated in 1/3 octave bands in responses reconstructed in the frequency range of 10 – 500 Hz for the small damping ratio.

OCV		Noise levels in operational responses			GCV		Noise levels in operational responses		
		Low	Medium	High			Low	Medium	High
Noise levels in FRF's	Low	0.1	3.4	3.8	Noise levels in FRF's	Low	0.1	3.7	7.7
	Medium	0.2	0.8	5.1		Medium	0.2	2.2	5.1
	High	1.6	1.4	2.4		High	1.5	1.2	2.5
MFE		Noise levels in operational responses			MRE		Noise levels in operational responses		
		Low	Medium	High			Low	Medium	High
Noise levels in FRF's	Low	0.1	0.7	0.9	Noise levels in FRF's	Low	0.1	0.4	0.2
	Medium	0.6	0.8	1.0		Medium	0.4	0.4	0.3
	High	1.1	1.2	1.4		High	0.8	0.8	0.5

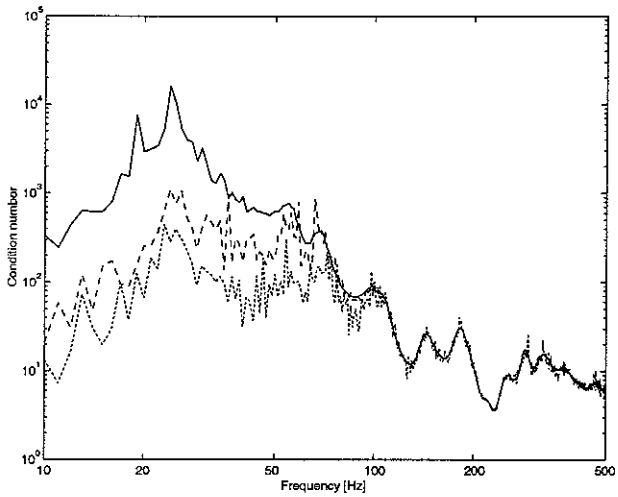

Figure 17. Condition numbers of the measured FRF's due to different levels of noise for the large damping ratio. —— low noise level, – – – medium, - - - - high.

Table 20. Average errors in dB calculated in 1/3 octave bands in forces reconstructed in the frequency range of 10 – 500 Hz for the large damping ratio.

OCV		Noise levels in operational responses			GCV		Noise levels in operational responses		
		Low	Medium	High			Low	Medium	High
Noise levels in FRF's	Low	1.9	6.7	6.5	Noise levels in FRF's	Low	1.8	11.1	15.8
	Medium	2.3	5.2	6.7		Medium	2.4	5.4	8.9
	High	2.7	2.8	5.1		High	2.8	3.1	6.0
MFE		Noise levels in operational responses			MRE		Noise levels in operational responses		
		Low	Medium	High			Low	Medium	High
Noise levels in FRF's	Low	0.3	1.5	2.1	Noise levels in FRF's	Low	1.6	7.5	11.2
	Medium	1.4	1.6	2.4		Medium	2.2	4.0	6.7
	High	1.9	2.0	2.6		High	2.7	3.1	4.8

Table 21. Average errors in dB calculated in 1/3 octave bands in responses reconstructed in the frequency range of 10 – 500 Hz for the large damping ratio.

OCV		Noise levels in operational responses			GCV		Noise levels in operational responses		
		Low	Medium	High			Low	Medium	High
Noise levels in FRF's	Low	0.2	2.3	3.2	Noise levels in FRF's	Low	0.1	3.5	8.3
	Medium	0.9	2.7	4.1		Medium	0.8	2.7	5.8
	High	0.6	1.5	1.9		High	0.6	0.9	2.5
MFE		Noise levels in operational responses			MRE		Noise levels in operational responses		
		Low	Medium	High			Low	Medium	High
Noise levels in FRF's	Low	0.1	0.6	1.3	Noise levels in FRF's	Low	0.1	0.3	0.2
	Medium	0.6	0.6	1.1		Medium	0.3	0.3	0.3
	High	1.0	1.2	1.3		High	0.5	0.5	0.3

5.4. Variation of the positions of applied forces

To investigate the relationship of force positions and the performance of OCV and GCV, five different distributions of force positions were used and their results were compared. The five distributions are as follows:

1) Existing distribution of force positions,
2) A distribution of force positions close to one another,
3) A distribution of force positions far from one another,
4) A distribution of force positions near to the response positions, and
5) A distribution of force positions coincident with the response positions.

Figure 18 and Table 22 show the non-dimensional positions of forces mentioned above and the response positions.

The close and far distributions of force positions are used to estimate effects of the relationship among force positions on the performance of OCV and GCV. The distributions near to and coincident with response positions are used to investigate effects of the relationship between force positions and response positions on the performance of two methods by comparing their results with those obtained from using the far distribution of force positions.

Table 22. Non-dimensional positions of various distributions of forces.

No	Force positions (x/a,y/b)					Force amplitudes [N]	Response positions (x/a,y/b)
	Existing distribution	Close to one another	Far from one another	Near to response positions	Coincident with response positions		
1	(0.41,0.43)	(0.38,0.26)	(0.11,0.26)	(0.62,0.49)	(0.60,0.50)	19	(0.55,0.40)
2	(0.51,0.63)	(0.43,0.30)	(0.89,0.95)	(0.92,0.84)	(0.90,0.80)	10	(0.90,0.80)
3	(0.62,0.41)	(0.42,0.25)	(0.78,0.14)	(0.63,0.34)	(0.61,0.31)	27	(0.60,0.50)
4	(0.31,0.72)	(0.40,0.32)	(0.33,0.87)	(0.70,0.68)	(0.70,0.71)	6	(0.70,0.71)
5							(0.61,0.31)

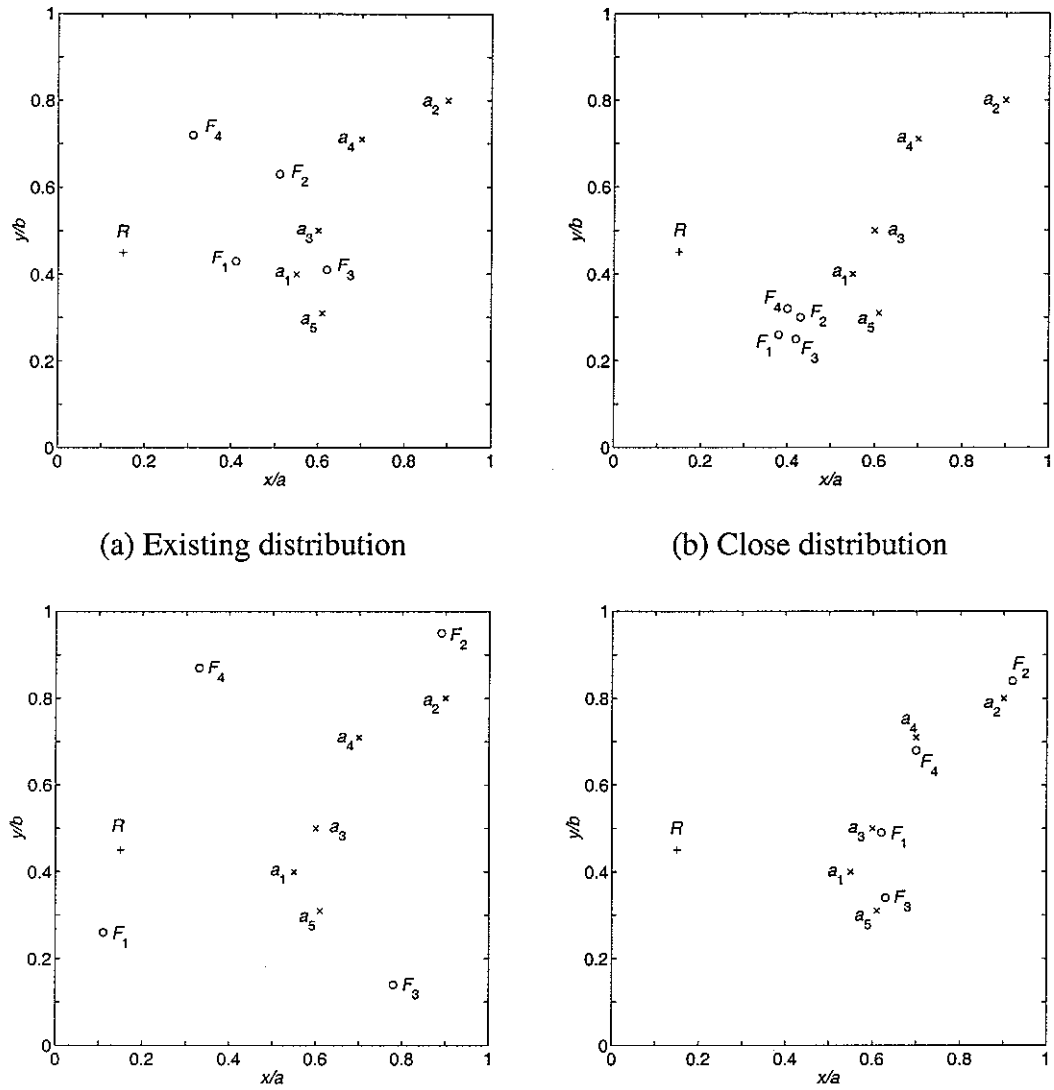

(a) Existing distribution

(b) Close distribution

(c) Far distribution

(d) Near to response positions

Figure 18. Various positions of forces. ○: force location, ×: response location, +: receiver location.

5.4.1. Close distribution

A distribution of force positions close to one another is obtained by choosing four points randomly within a circle of non-dimensional diameter 0.1, see Figure 18 (b).

The average errors in reconstructed forces and responses are given in Tables 23 and 24, respectively. Force errors become larger than those obtained from the existing distribution (Tables 12 and 13). This is because the condition numbers of the FRF's are worse, as shown in Figure 19, and it is difficult to distinguish forces due to the

interference between close force positions. However, in spite of the increased force errors, the response errors decrease generally. This may be due to the concentration of the forces. Therefore the transfer functions from force positions to receiver positions are very similar and then because of the interference of similar transfer functions the response errors become less.

In this case OCV gives better or equal force and response estimates than GCV for all 9 noise level combinations.

5.4.2. Far distribution

Four points were selected from many points generated randomly, such that they were each at least a non-dimensional distance 0.5 from one another. They are shown in Figure 18 (c). Tables 25 and 26 give the average errors in reconstructed forces and responses, respectively. The condition numbers are plotted in Figure 20. Comparing these results with those of the original and close distributions, the force errors decrease for low noise levels in FRF's. This can be related to the fact that the FRF condition numbers reduce. Also in the case of medium noise level in FRF's with high noise level in operational responses the force errors decrease.

Comparing the results of the close distribution with those of the far distribution, the force errors of the far distribution are less than those of the close distribution. This is because the interference among the forces reduces considerably due to the increase of the distances between them. For the same reason, the condition numbers of the frequency response function matrices for the far distribution become smaller than those for the close distribution. The response errors are at a similar level except for those for the low noise level in FRF's with high noise level in operational responses.

The differences between OCV and GCV are smaller in this case, but the results for OCV remain slightly better than for GCV.

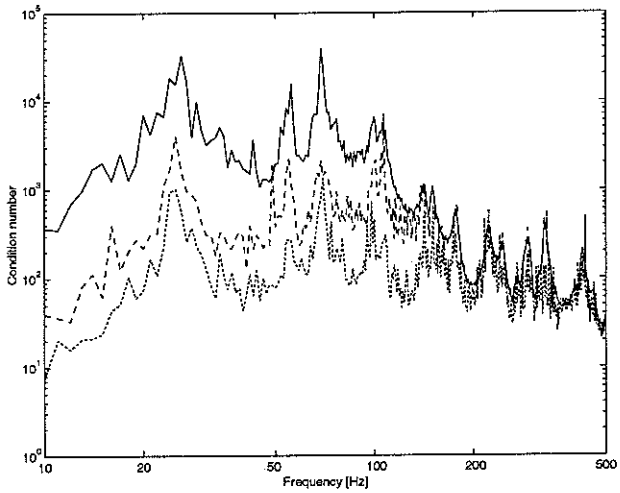

Figure 19. Condition numbers of the measured FRF's due to different levels of noise for the close distribution of forces. —— low noise level, – – – medium, - - - - high.

Table 23. Average errors in dB calculated in 1/3 octave bands in forces reconstructed in the frequency range of 10 – 500 Hz for the close distribution of forces.

OCV		Noise levels in operational responses			GCV		Noise levels in operational responses		
		Low	Medium	High			Low	Medium	High
Noise levels in FRF's	Low	1.9	14.3	22.3	Noise levels in FRF's	Low	2.2	17.6	29.8
	Medium	4.1	6.5	12.8		Medium	4.1	7.8	14.8
	High	4.2	4.9	7.5		High	4.3	5.1	7.9
MFE		Noise levels in operational responses			MRE		Noise levels in operational responses		
		Low	Medium	High			Low	Medium	High
Noise levels in FRF's	Low	1.5	3.1	3.3	Noise levels in FRF's	Low	3.1	12.7	18.7
	Medium	3.2	3.1	3.4		Medium	3.8	6.6	9.9
	High	3.3	3.4	3.4		High	4.4	4.7	6.2

Table 24. Average errors in dB calculated in 1/3 octave bands in responses reconstructed in the frequency range of 10 – 500 Hz for the close distribution of positions.

OCV		Noise levels in operational responses			GCV		Noise levels in operational responses		
		Low	Medium	High			Low	Medium	High
Noise levels in FRF's	Low	0.1	1.7	5.6	Noise levels in FRF's	Low	0.1	2.4	7.3
	Medium	0.1	0.1	0.6		Medium	0.1	0.1	1.1
	High	0.2	0.3	0.6		High	0.2	0.3	0.6
MFE		Noise levels in operational responses			MRE		Noise levels in operational responses		
		Low	Medium	High			Low	Medium	High
Noise levels in FRF's	Low	0.1	0.4	0.4	Noise levels in FRF's	Low	0.0	0.0	0.1
	Medium	0.3	0.4	0.4		Medium	0.0	0.0	0.1
	High	0.5	0.5	0.7		High	0.1	0.1	0.1

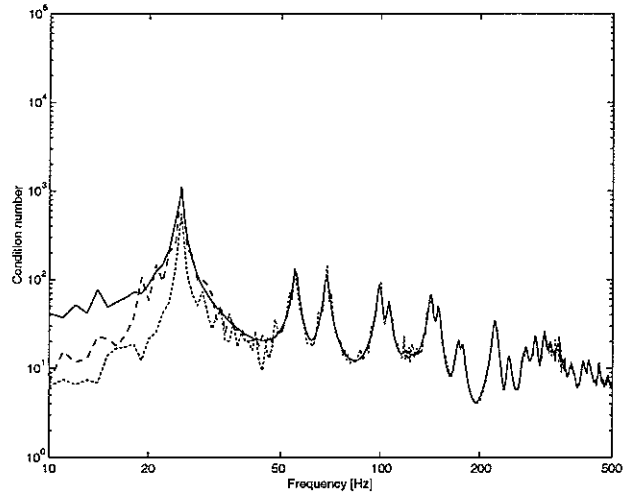

Figure 20. Condition numbers of the measured FRF's due to different levels of noise for the far distribution of forces. —— low noise level, – – – medium, - - - - high.

Table 25. Average errors in dB calculated in 1/3 octave bands in forces reconstructed in the frequency range of 10 – 500 Hz for the far distribution of force positions.

OCV		Noise levels in operational responses			GCV		Noise levels in operational responses		
		Low	Medium	High			Low	Medium	High
Noise levels in FRF's	Low	0.8	5.2	7.4	Noise levels in FRF's	Low	0.9	6.2	7.6
	Medium	2.9	4.0	4.9		Medium	2.9	5.0	5.4
	High	2.9	2.9	5.6		High	2.7	3.0	6.2
MFE		Noise levels in operational responses			MRE		Noise levels in operational responses		
		Low	Medium	High			Low	Medium	High
Noise levels in FRF's	Low	0.5	2.1	2.7	Noise levels in FRF's	Low	2.4	5.4	5.5
	Medium	1.7	1.9	2.5		Medium	3.0	3.7	5.1
	High	2.1	2.3	2.7		High	3.1	3.6	4.0

Table 26. Average errors in dB calculated in 1/3 octave bands in responses reconstructed in the frequency range of 10–500 Hz for the far distribution of force positions.

OCV		Noise levels in operational responses			GCV		Noise levels in operational responses		
		Low	Medium	High			Low	Medium	High
Noise levels in FRF's	Low	0.3	1.6	1.9	Noise levels in FRF's	Low	0.2	2.1	3.0
	Medium	0.2	0.8	1.3		Medium	0.2	1.1	2.6
	High	1.0	1.7	3.1		High	0.9	1.8	3.6
MFE		Noise levels in operational responses			MRE		Noise levels in operational responses		
		Low	Medium	High			Low	Medium	High
Noise levels in FRF's	Low	0.3	0.7	1.3	Noise levels in FRF's	Low	0.1	0.3	0.3
	Medium	0.2	0.9	1.2		Medium	0.2	0.3	0.3
	High	0.8	1.3	1.2		High	0.4	0.6	0.4

5.4.3. Force positions near to response positions

A distribution of force positions is made by generating points randomly within a radius of 0.05 for each response point. The 1st, 2nd, 3rd, and 4th force positions are near to the 3rd, 2nd, 5th, and 4th response positions, respectively, see Figure 18 (d).

Tables 27 and 28 show the results of the average errors in reconstructed forces and responses, respectively. The condition numbers are given in Figure 21. Comparing these results with those in the original case (Tables 12 and 13), the force errors for low and medium noise levels in FRF's decrease very much because the condition numbers for these noise levels reduce considerably, but for high noise level in FRF's the condition numbers are similar to those of the original distribution. The errors in the responses reconstructed also become much smaller except for medium noise level in FRF's with high noise level in operational responses, in which case the response error at about 10 Hz is magnified.

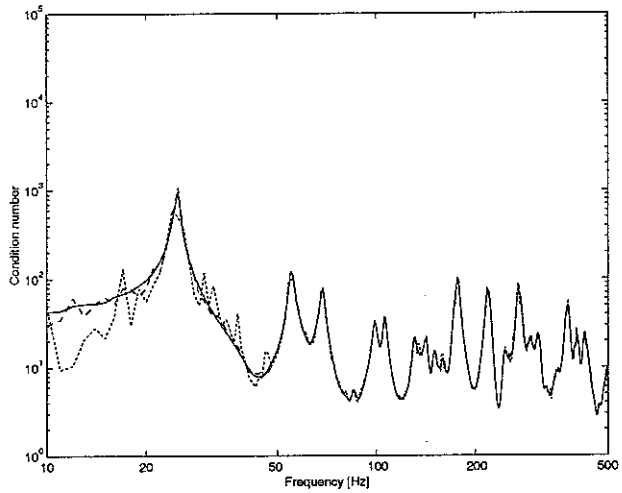

Figure 21. Condition numbers of the measured FRF's due to different levels of noise for the distribution of force positions near to response positions. —— low noise level, – – – medium, - - - - high.

Comparing these results with those for the far distribution, in which the distances between force positions and responses are larger than here, the errors in forces and responses generally decrease in the present case.

In the present case OCV still generally gives better results than GCV although the differences are small.

Table 27. Average errors in dB calculated in 1/3 octave bands in forces reconstructed in the frequency range of 10 – 500 Hz for the distribution of force positions near to response positions.

OCV		Noise levels in operational responses			GCV		Noise levels in operational responses		
		Low	Medium	High			Low	Medium	High
Noise levels in FRF's	Low	0.2	2.9	6.1	Noise levels in FRF's	Low	0.2	3.0	6.2
	Medium	1.5	2.4	6.9		Medium	1.4	2.2	7.4
	High	2.8	3.2	3.2		High	2.8	3.0	5.8
MFE		Noise levels in operational responses			MRE		Noise levels in operational responses		
		Low	Medium	High			Low	Medium	High
Noise levels in FRF's	Low	0.2	1.6	2.2	Noise levels in FRF's	Low	1.8	2.8	3.5
	Medium	1.1	1.8	2.2		Medium	2.0	3.2	3.6
	High	1.7	2.0	2.3		High	2.7	3.1	3.5

Table 28. Average errors in dB calculated in 1/3 octave bands in responses reconstructed in the frequency range of 10 – 500 Hz for the distribution of force positions near to response positions.

OCV		Noise levels in operational responses			GCV		Noise levels in operational responses		
		Low	Medium	High			Low	Medium	High
Noise levels in FRF's	Low	0.1	0.2	0.6	Noise levels in FRF's	Low	0.1	0.1	0.5
	Medium	0.1	0.3	2.4		Medium	0.1	0.1	2.9
	High	0.2	0.3	0.5		High	0.1	0.3	0.8
MFE		Noise levels in operational responses			MRE		Noise levels in operational responses		
		Low	Medium	High			Low	Medium	High
Noise levels in FRF's	Low	0.1	0.1	0.3	Noise levels in FRF's	Low	0.1	0.1	0.3
	Medium	0.1	0.1	0.3		Medium	0.1	0.1	0.3
	High	0.2	0.3	0.4		High	0.1	0.2	0.3

5.4.4. Force positions coincident with response positions

Tables 29 and 30 give results for force positions coincident with the response positions. Figure 22 gives the condition numbers.

Comparing this case with the previous case, the results are very similar or identical. The errors of results identified for this distribution are less than or equal to those in the previous one because the variation of force positions is relatively small.

In conclusion, the performance of force and response reconstruction using a far distribution of force positions is better than those using a close distribution when not considering force and response positions altogether. However if considering all positions of forces and responses, force positions near to response positions are more beneficial. In each case OCV gives better results than GCV, although as the results improve the difference between the methods becomes less.

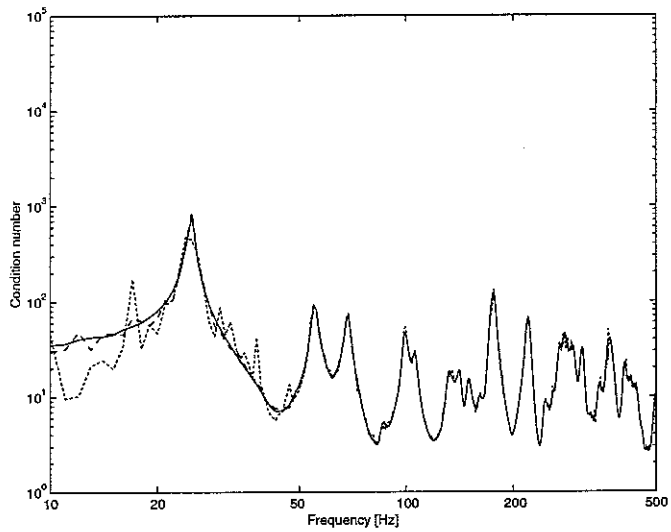

Figure 22. Condition numbers of the measured FRF's due to different levels of noise for the distribution of force positions coincident with response positions. —— low noise level, – – – medium, - - - - high.

Table 29. Average errors in dB calculated in 1/3 octave bands in forces reconstructed in the frequency range of 10 – 500 Hz for the distribution of force positions coincident with response positions.

OCV		Noise levels in operational responses			GCV		Noise levels in operational responses		
		Low	Medium	High			Low	Medium	High
Noise levels in FRF's	Low	0.2	2.6	5.4	Noise levels in FRF's	Low	0.2	2.8	5.5
	Medium	1.4	1.8	6.3		Medium	1.5	2.0	6.7
	High	2.6	2.9	2.8		High	2.6	3.2	2.8
MFE		Noise levels in operational responses			MRE		Noise levels in operational responses		
		Low	Medium	High			Low	Medium	High
Noise levels in FRF's	Low	0.2	1.5	2.1	Noise levels in FRF's	Low	1.5	2.5	3.3
	Medium	1.1	1.8	2.1		Medium	1.9	3.1	4.3
	High	1.6	1.9	2.1		High	2.3	2.9	3.6

Table 30. Average errors in dB calculated in 1/3 octave bands in responses reconstructed in the frequency range of 10 – 500 Hz for the distribution of force positions coincident with response positions.

OCV		Noise levels in operational responses			GCV		Noise levels in operational responses		
		Low	Medium	High			Low	Medium	High
Noise levels in FRF's	Low	0.1	0.2	1.0	Noise levels in FRF's	Low	0.1	0.1	0.9
	Medium	0.2	0.2	2.1		Medium	0.2	0.1	2.1
	High	0.2	0.2	0.8		High	0.2	0.3	0.7
MFE		Noise levels in operational responses			MRE		Noise levels in operational responses		
		Low	Medium	High			Low	Medium	High
Noise levels in FRF's	Low	0.1	0.2	0.9	Noise levels in FRF's	Low	0.1	0.2	0.3
	Medium	0.1	0.2	0.9		Medium	0.1	0.1	0.3
	High	0.2	0.3	0.8		High	0.2	0.2	0.3

6. VARIATION OF THE SIGNAL-TO-NOISE RATIO IN FRF'S AND IN OPERATIONAL RESPONSES

6.1. Introduction

In this section, the performance of OCV and GCV for reconstructing forces is considered for a large range of the noise levels, that is the signal-to-noise (S/N) ratios of the FRF's and measured operational responses.

To investigate effects of only noise in signals on the performance of the two methods, other factors need to be excluded. Therefore, firstly exact frequency response functions and operational responses with no noise are calculated, and random noise with proper S/N ratios is added to the exact signals. Then from the measured signals with known noise levels, the reconstruction of forces is conducted by using the methods of OCV and GCV, and their performances are compared with respect to the S/N ratio. This procedure is summarized as follows:

1) Calculate exact frequency response functions $\overline{H}(\omega)$ and operational responses $\overline{a}(\omega)$ without noise.
2) Generate noise models such as

$$N(\omega) = \omega N_{nd} e^{j2\pi N_{ud}}, \tag{21}$$

where N_{nd} is normally distributed random number with mean 0 and standard deviation 1 and N_{ud} is uniformly distributed random number in the range from 0 to 1.

3) Adjust noise models to give specific S/N ratio such as

$$\hat{N}(\omega,\varepsilon) = N(\omega)\frac{|S(\omega)|}{|N(\omega)|}\varepsilon, \tag{22}$$

where $S(\omega)$ is $\overline{H}(\omega)$ or $\overline{a}(\omega)$, ε is a S/N ratio, and $|\cdot|$ is a 2-norm in matrices or the Frobenius norm in vectors.

4) Add noise to signals and make measured FRF's and responses

$$\begin{aligned} \hat{H}(\omega,\varepsilon) &= \overline{H}(\omega) + \hat{N}_H(\omega,\varepsilon) \\ \hat{a}(\omega,\varepsilon) &= \overline{a}(\omega) + \hat{N}_a(\omega,\varepsilon) \end{aligned} \tag{23}$$

where $\hat{N}_H(\omega,\varepsilon)$ and $\hat{N}_a(\omega,\varepsilon)$ are respective noise values with specific S/N ratio.

5) Repeat the above steps 2 to 4 for different values of S/N ratio.

6) Reconstruct forces and responses by using OCV and GCV.

6.2. Effect of S/N ratio on the performance of OCV and GCV

In this study, a series of S/N ratio are used between -40 dB and -10 dB with a step of 1 dB. The S/N ratio of -40 dB corresponds to a low noise level and that of -10 dB corresponds to a high noise level. Figure 23 shows an example of the exact signals and noise with S/N ratio of -40 dB. The noise here differs from that considered earlier in this report by the fact that it is proportional to the signal at every frequency. Note also that only single noise samples are used, whereas previously averaging was performed in obtaining 'measured' FRF's and operational responses.

Using the measured frequency response functions and operational responses with S/N ratio of -40 dB to -10 dB with a step of 1 dB, the average errors of forces are calculated by using three methods: OCV, GCV, and MFE (minimum force error). These were carried out under four conditions:

1) low noise level (S/N ratio of -40 dB) in FRF's, variable noise in operational responses,

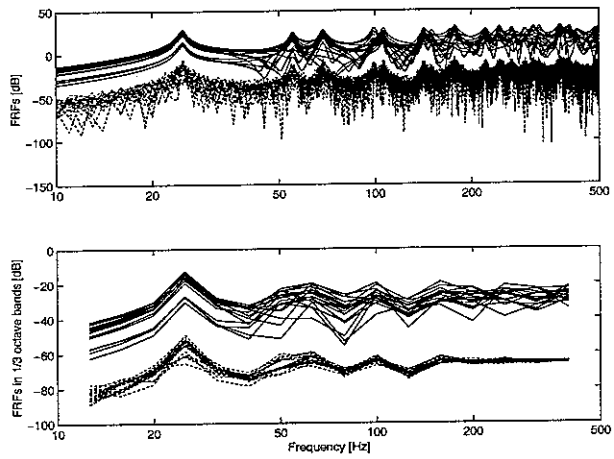

(a) FRF's

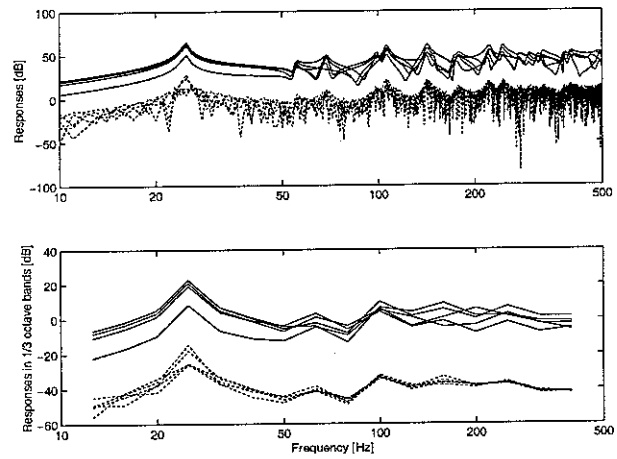

(b) Operational responses

Figure 23. Comparisons of responses and noise with the S/N ratio of – 40 dB.
—— signal, - - - - noise.

2) high noise level (S/N ratio of – 10 dB) in FRF's, variable noise in operational responses,
3) low noise level (S/N ratio of – 40 dB) in operational responses, variable noise in FRF's, and
4) high noise level (S/N ratio of – 10 dB) in operational responses, variable noise in FRF's.

Figures 24 to 27 shows the average errors in reconstructed forces and in regularization parameters selected as optimal values in each condition mentioned

above. Here 10 sets of results of reconstructed forces and regularization parameters are obtained from 10 different sets of measured frequency response functions and operational responses. The average result from these 10 cases is presented in the figures (NB This differs from using the average FRF and responses in determining the forces).

The average errors in the forces in these figures are defined as the root mean square error (RMSE) between the forces obtained by OCV (or GCV) and the forces obtained by MFE and are written as

$$\Delta F_{method} = \frac{1}{m}\sum_{i=1}^{m}\sqrt{\frac{1}{n}\sum_{j=1}^{n}\left(20\log\left|F^{(i)}_{method,j}\right| - 20\log\left|F^{(i)}_{MFE,j}\right|\right)^2}\,, \tag{24}$$

where *method* is OCV or GCV, m is the number of result sets (here 10), and n is the number of forces (4). Similarly the average errors in optimal regularization parameters are defined as the average of the differences between those obtained by OCV (or GCV) and those obtained by MFE in logarithmic scale and are written as

$$\Delta\lambda_{method} = \frac{1}{m}\sum_{i=1}^{m}\left|\log\lambda^{(i)}_{method} - \log\lambda^{(i)}_{MFE}\right|. \tag{25}$$

For low noise level in the FRF's (see Figure 24), the force errors are small in the frequency range above 100 Hz and in this range noise effects are relatively small. In the frequency range below 50 Hz the force errors are small only for low noise levels in the operational responses. For OCV, a high error exists around 55 Hz regardless of the noise level in the operational responses, which is not present for GCV. The errors in the regularization parameters show a somewhat reversed trend compared with the trend of the force errors. Thus at high frequencies and low noise level, the methods may give large differences in optimal regularization parameters but this has little effect on the forces.

As shown in Figures 24 to 27, the comparison of the results by the two methods is difficult because the results are similar to each other. Therefore, other plots are needed to be able to compare the performance of OCV and GCV more easily. Figures 28 and 29 show the differences between the average errors by OCV and by GCV in forces and in optimal regularization parameters. These figures show the dominant area of each method. The concept to separate the regions where OCV or GCV gives better results is defined as

$$\begin{aligned} &\text{OCV better:} \quad \Delta F_{OCV} - \Delta F_{GCV} \leq -1\,\text{dB}, \\ &\text{Similar:} \quad \left|\Delta F_{OCV} - \Delta F_{GCV}\right| < +1\,\text{dB}, \\ &\text{GCV better:} \quad \Delta F_{OCV} - \Delta F_{GCV} \geq +1\,\text{dB}. \end{aligned} \tag{26}$$

From Figure 28, OCV is seen to be better than GCV in the low frequency region below 50 Hz and around 100 Hz and GCV is better around 50 Hz and above 100 Hz.

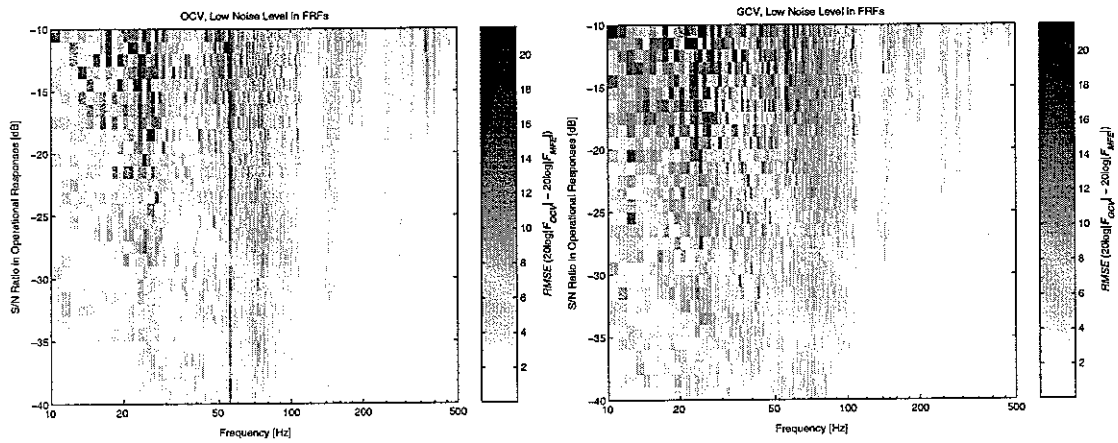

(a) ΔF_{OCV} (b) ΔF_{GCV}

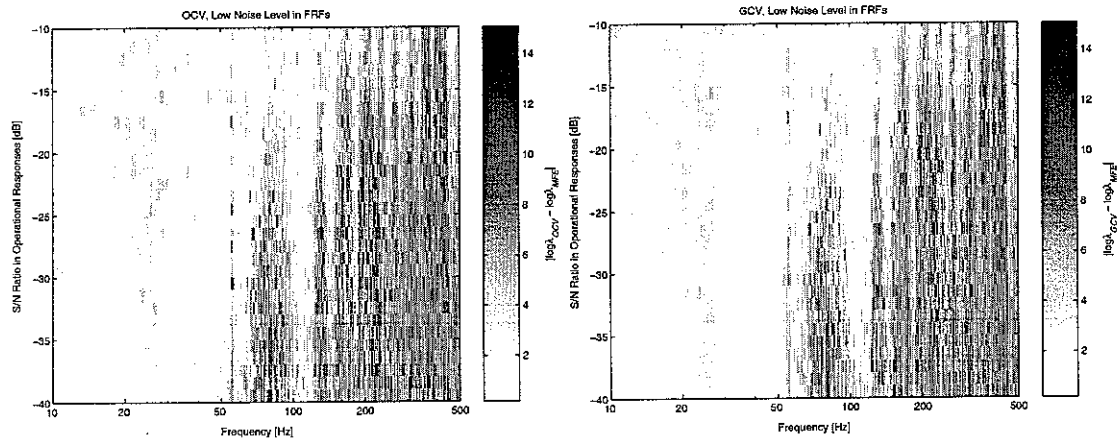

(c) $\Delta\lambda_{OCV}$ (d) $\Delta\lambda_{GCV}$

Figure 24. Average errors in forces reconstructed and regularization parameters selected for low noise level in FRF's and variable S/N ratio in operational responses.

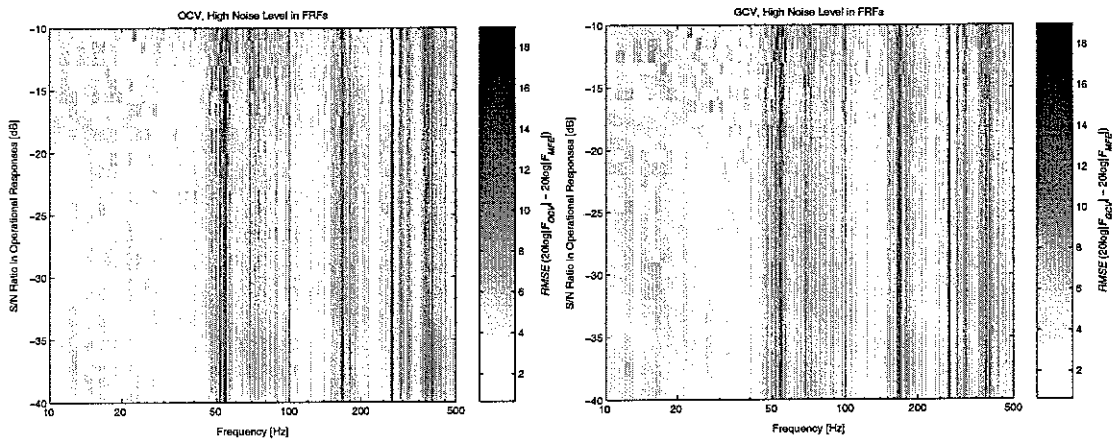

(a) ΔF_{OCV} (b) ΔF_{GCV}

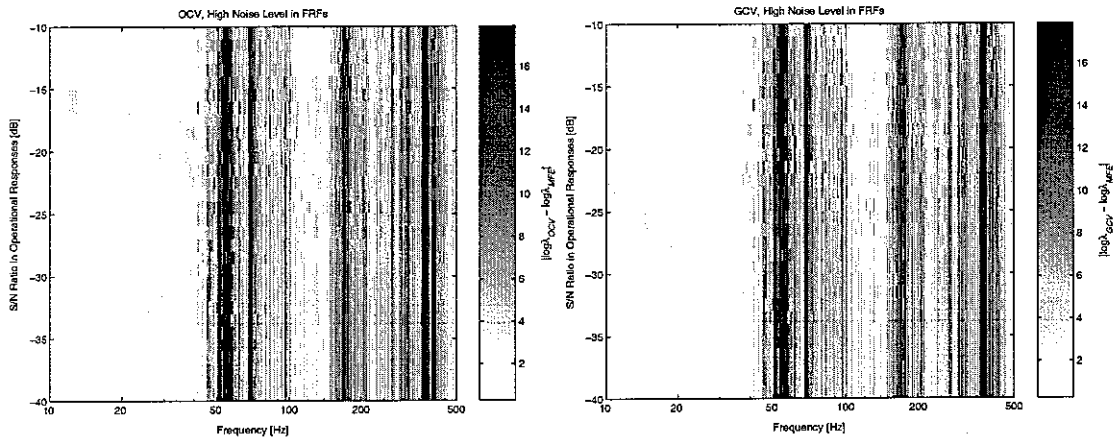

(c) $\Delta\lambda_{OCV}$ (d) $\Delta\lambda_{GCV}$

Figure 25. Average errors in forces reconstructed and regularization parameters selected for high noise level in FRF's and variable S/N ratio in operational responses.

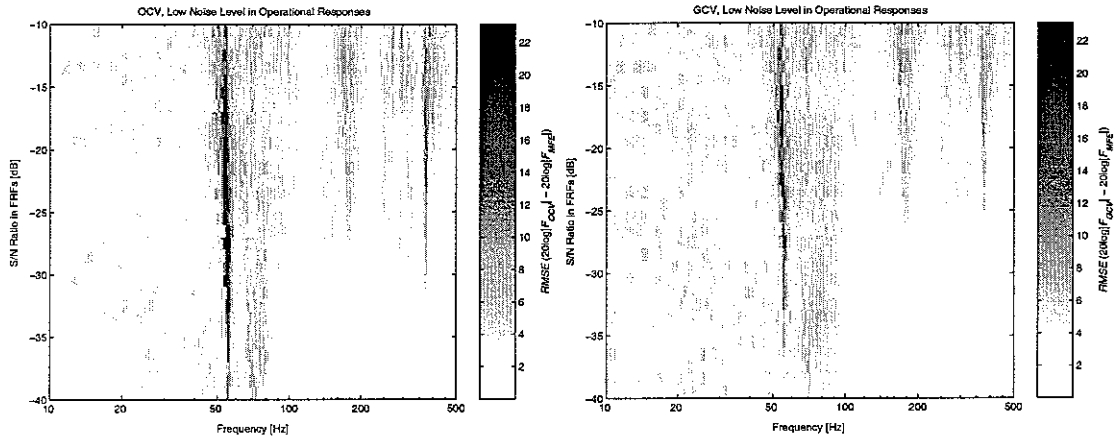

(a) ΔF_{OCV} (b) ΔF_{GCV}

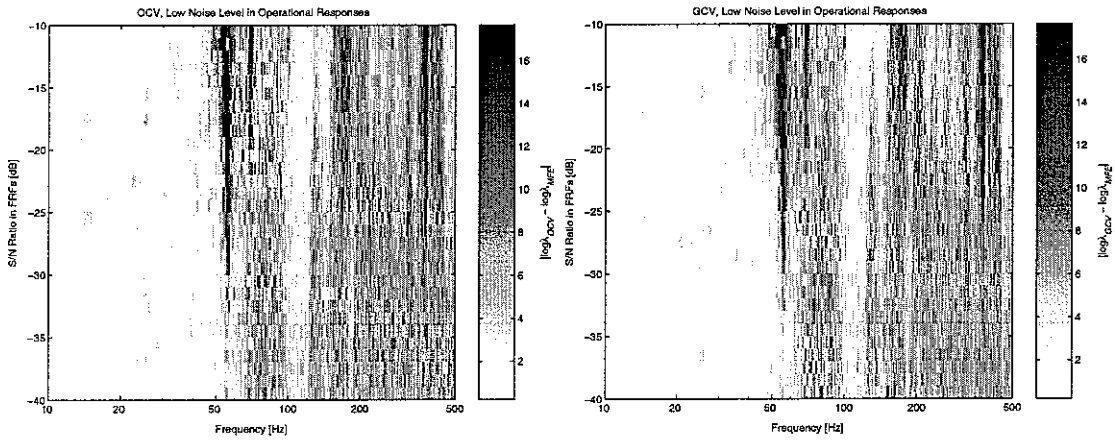

(c) $\Delta\lambda_{OCV}$ (d) $\Delta\lambda_{GCV}$

Figure 26. Average errors in forces reconstructed and regularization parameters selected for low noise level in operational responses and variable S/N ratio in FRF's.

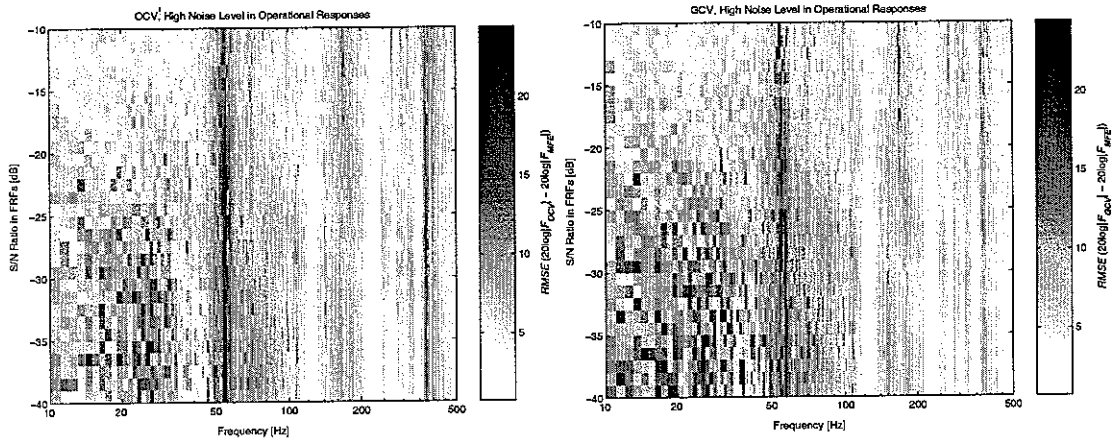

(a) ΔF_{OCV} (b) ΔF_{GCV}

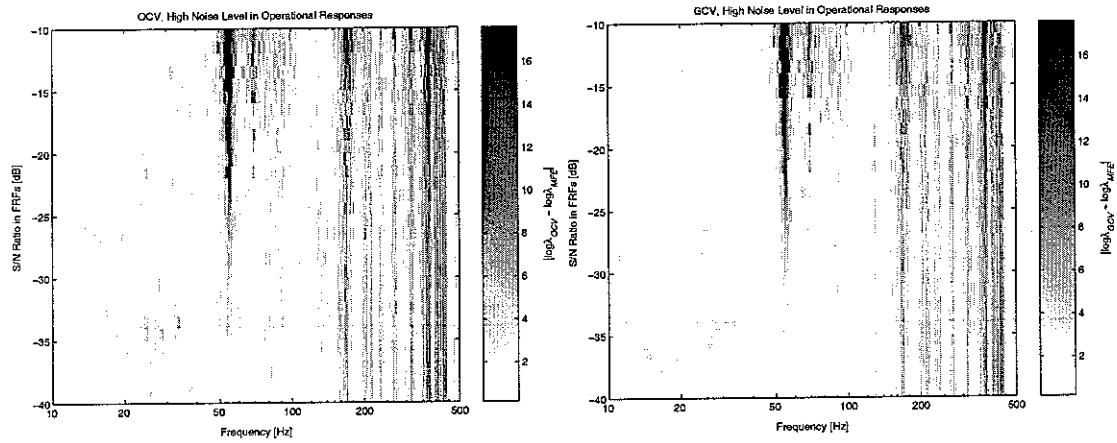

(c) $\Delta \lambda_{OCV}$ (d) $\Delta \lambda_{GCV}$

Figure 27. Average errors in forces reconstructed and regularization parameters selected for high noise level in operational responses and variable S/N ratio in FRF's.

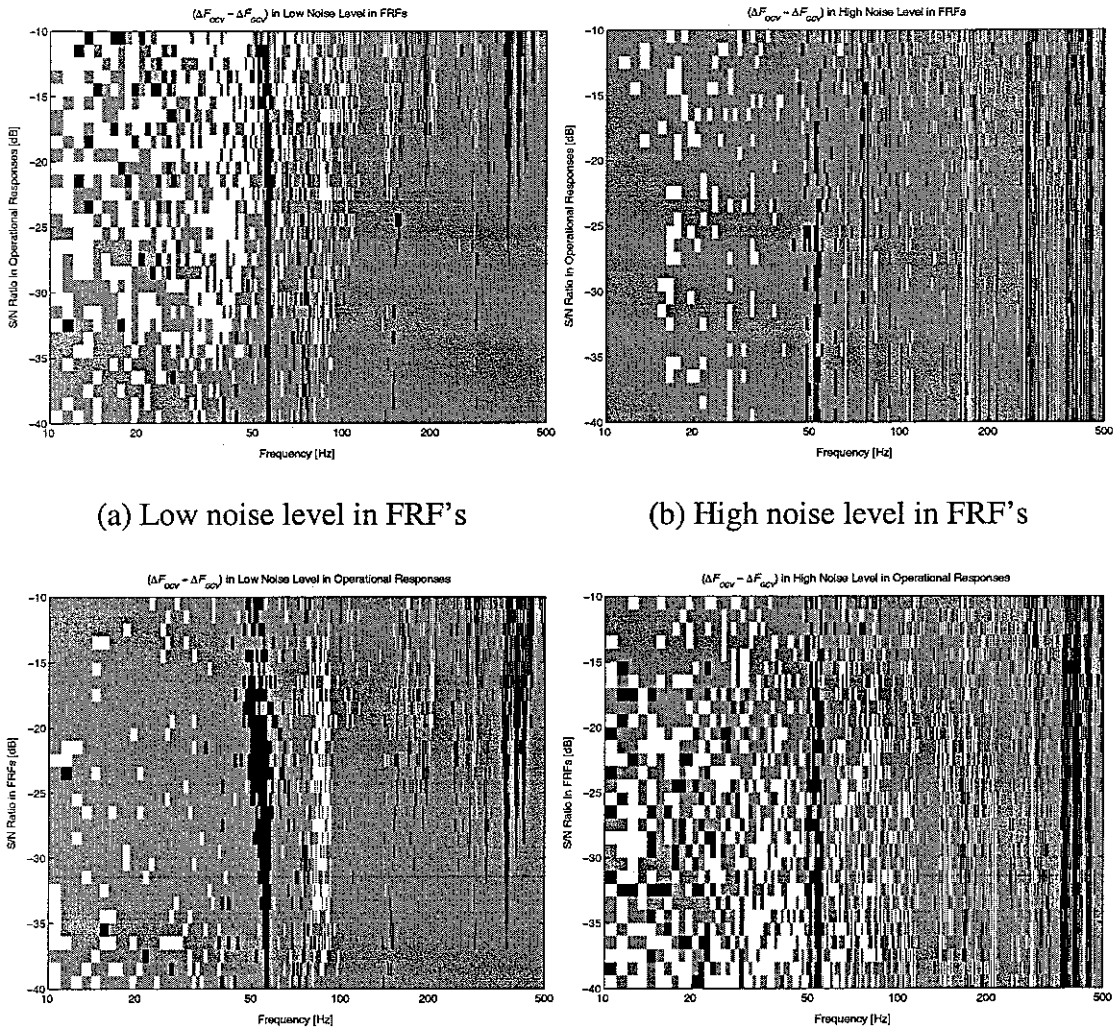

(a) Low noise level in FRF's

(b) High noise level in FRF's

(c) Low noise level in responses

(d) High noise level in responses

Figure 28. Comparison of average errors in forces reconstructed by OCV and GCV for various noise levels in operational responses and FRF's.

□: OCV better, ▩: same, ■: GCV better.

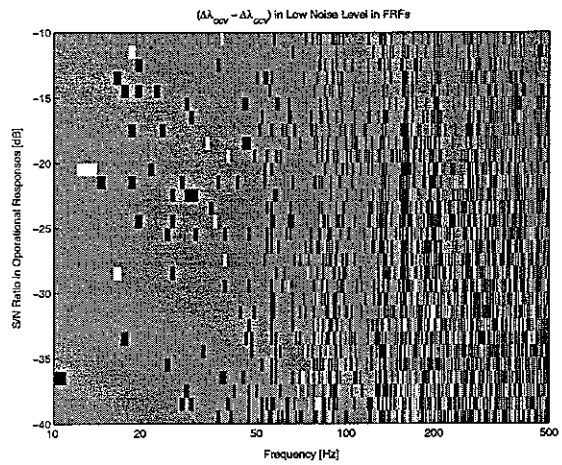

(a) Low noise level in FRF's

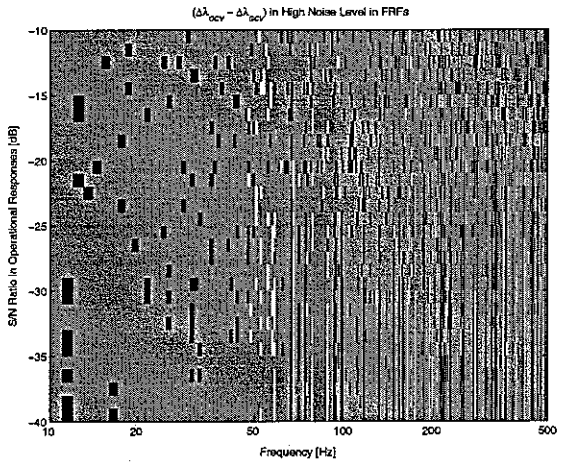

(b) High noise level in FRF's

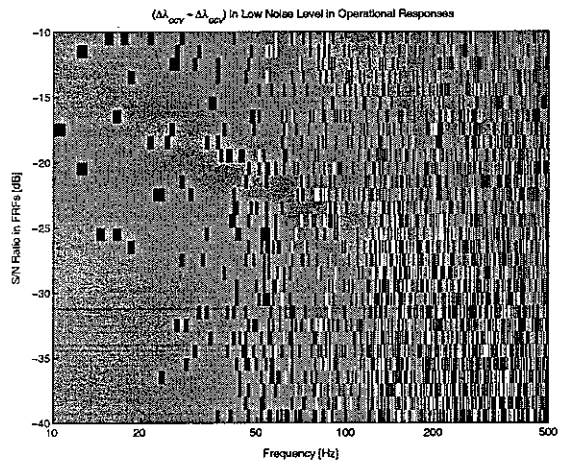

(c) Low noise level in responses

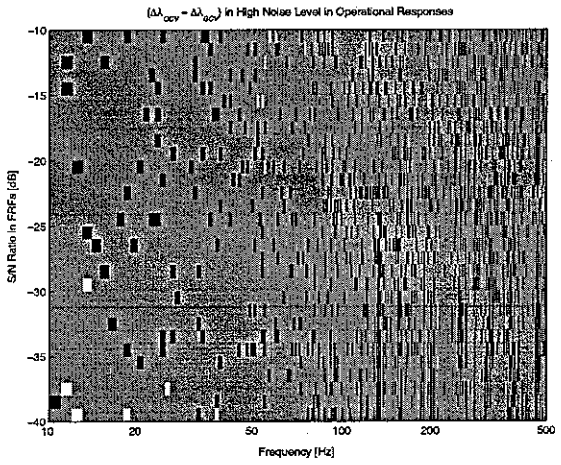

(d) High noise level in responses

Figure 29. Comparison of average errors in regularization parameters selected by OCV and GCV for various noise levels in operational responses and FRF's.
□: OCV better, ▩: same, ■: GCV better.

For some frequencies at which GCV is better than OCV in Figure 28, the validation functions of OCV and GCV are plotted in Figure 30. The results shown in Figures 24 to 29 are obtained from 10 different sets of data. In Figure 30 two examples of each are given. The validation functions in each case show different curves and different optimal regularization parameters for OCV and GCV. The squared singular values are also shown in Figure 30 but these have no consistent

relationship with the minima in the validation functions. The presence of two local minima in the validation functions at 55 Hz appears to be the cause of the poor results for OCV at this frequency. However the reason for this feature could not be established.

As shown in Figure 28, it is difficult to estimate the superiority between OCV and GCV in the full frequency range because of the variation of the performance of the two methods with respect to the frequencies. Thus a new value to represent the superiority at each S/N ratio under each noise condition is needed. The average of the results in Figure 28 is first calculated in each 1/3 octave band. Then the average over all 1/3 octave bands is formed. For calculating this average, the white areas where OCV is better than GCV a value of +1 is taken, the black areas where GCV is better than OCV a value of –1 is taken, and the grey is allocated a value of 0. So if the average is positive then OCV is better than GCV, and if that is negative then GCV is better than OCV.

Figure 31 shows the results of this comparison of the average errors in reconstructed forces obtained by OCV and GCV. It can be seen that OCV is better than GCV for low noise levels in FRF's without regard to S/N ratios in operational responses and also for high noise levels in operational responses without regard to S/N ratios in FRF's. However in the case of high noise levels in FRF's and in the case of low noise levels in operational responses, no consistent difference is found between the methods so that the performance of OCV and GCV is similar in these conditions. Therefore these results from Figure 31 are consistent with previous results, see for example Table 4.

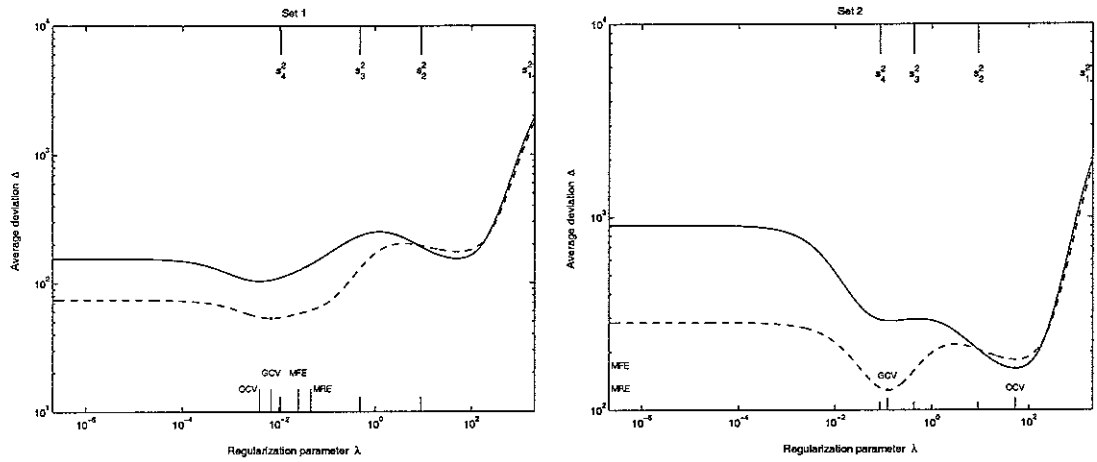

(a) 55 Hz

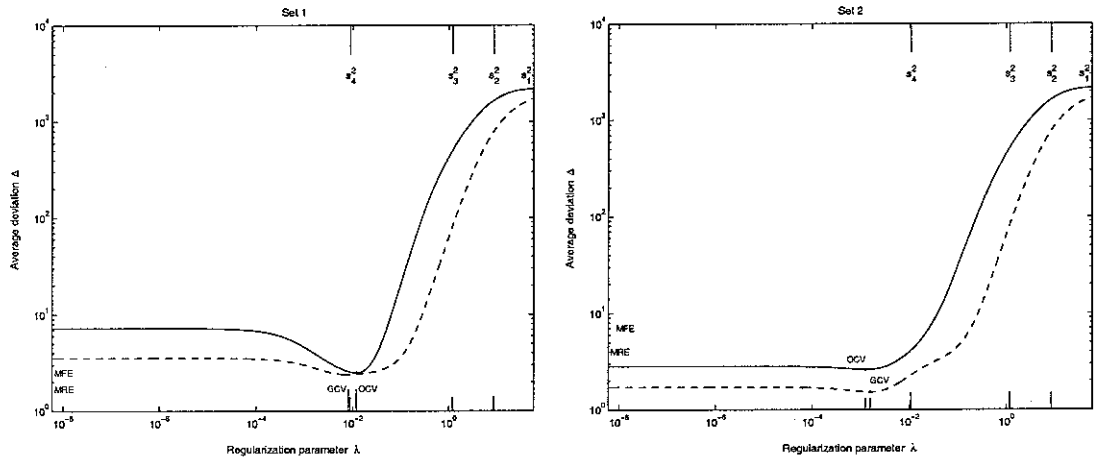

(b) 85 Hz

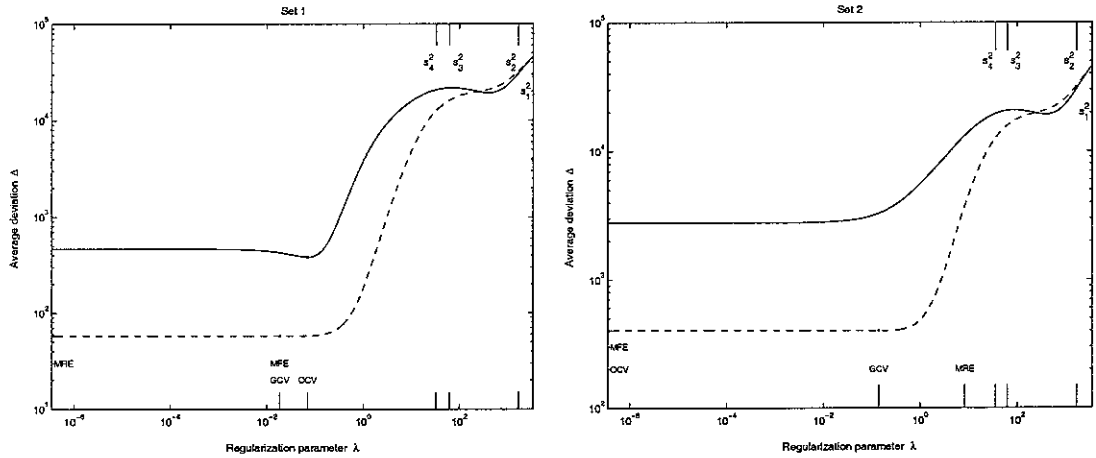

(c) 400 Hz

Figure 30. Validation functions against regularization parameters for the methods of OCV and GCV at specific frequencies in low noise levels in FRF's and operational responses. —— OCV, – – – GCV.

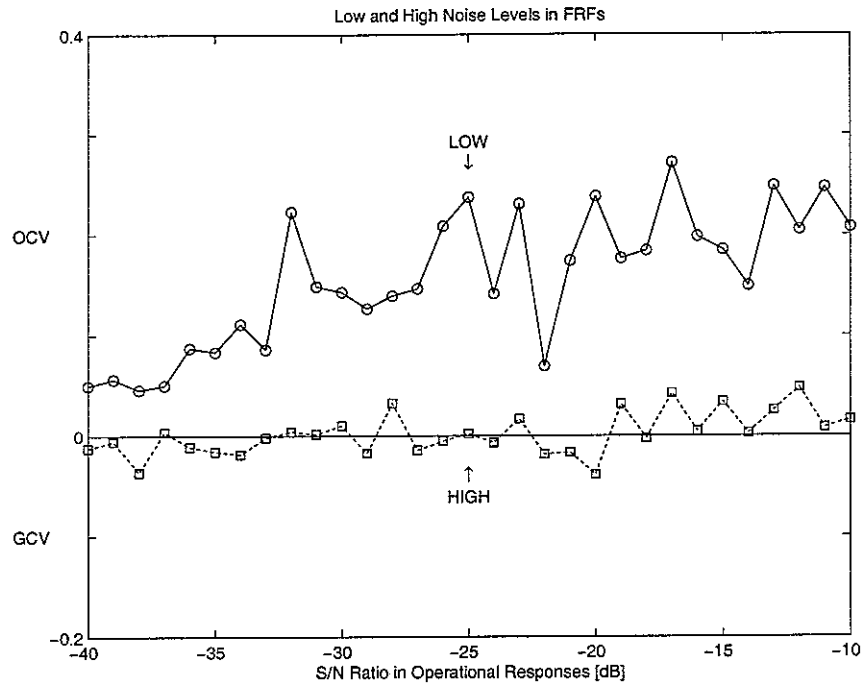

(a) Low and high noise levels in FRF's

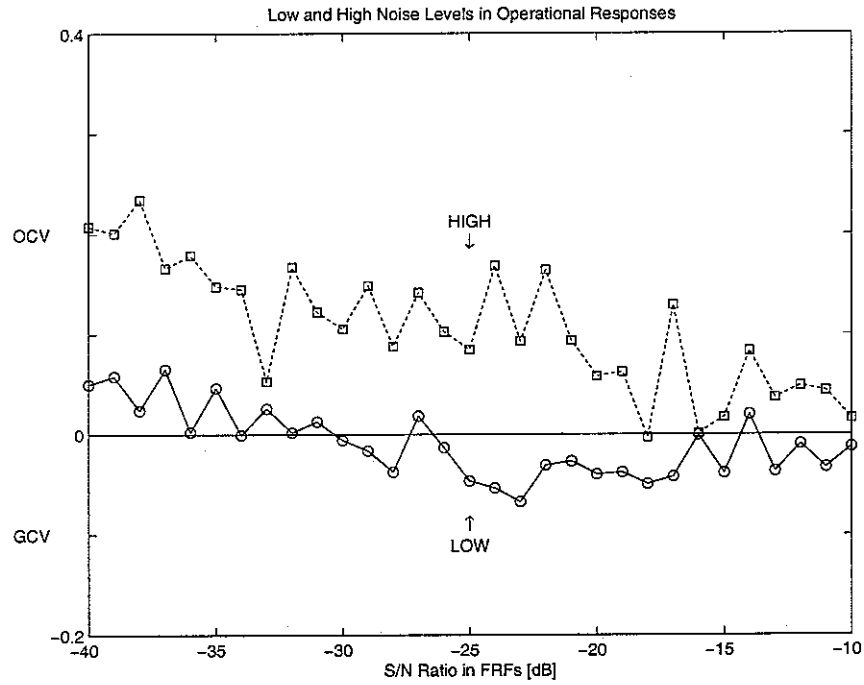

(b) Low and high noise levels in operational responses

Figure 31. The average calculated in 1/3 octave bands of the force errors reconstructed by OCV and by GCV for various noise levels in operational responses and FRF's.

7. CONCLUSIONS

In this study, the method of generalized cross validation was investigated in order to apply this method to structural dynamics problems. For a rectangular flat plate, the forces and responses were reconstructed by ordinary cross validation, selective cross validation, generalized cross validation based on OCV and a variant based on SCV, minimum force error, and minimum response error. From the average errors of forces and responses reconstructed by each method, it can be seen that the method of ordinary cross validation is generally more reliable than the other methods considered except the ideal methods of minimum force error and of minimum response error. The robustness of these methods was investigated for different noise levels in FRF's and in operational responses. The method of generalized cross validation based on ordinary cross validation is better at high frequencies (where condition numbers are low) but worse than OCV at low frequencies. A merit of generalized cross validation is that in the present results 0 is not chosen as a regularization parameter, whereas with OCV this is often the case. However this can be overcome by limiting the allowable range.

The optimal range of regularization parameters used for each method was investigated. An initial full range between 0 and the largest singular value squared was used, but this range is too wide for general use. Therefore a narrower range is needed. For the upper limit, the largest singular value squared appears reasonable. The norm of the error matrix and the smallest singular value squared are considered as the lower limit. From simulations for several ranges of regularization parameters, it is concluded that the minimum of these two values should be used as the lower limit.

The effects of some factors described in chapter 5 on the performance of the methods of OCV and GCV were evaluated. For the shape of plates, the square plate is

found to have smaller errors than a rectangular plate. A small damping ratio gives better performance for low noise levels in operational responses whereas a large damping ratio gives better performance for high noise levels in operational responses. However this will not necessarily always apply to other damping ratios. For the positions of forces, a distribution of forces far from one another allows better reconstructions than a distribution of forces close to one another. Moreover a distribution near to response positions gives better performance using either OCV or GCV. For all these cases OCV and GCV show fairly similar results with low and medium noise levels in operational responses but OCV is usually better than GCV for high noise levels in operational responses.

Finally, results have been obtained for a large range of noise levels added to the FRF's and operational responses. Generally OCV has a better performance at low frequencies, while GCV is better at high frequencies. However, since the need for regularization in the present problem is greater at low frequencies, where the condition numbers are high, it is found that OCV gives more reliable results than GCV.

REFERENCES

1. M. H. A. Janssens, J. W. Verheij, and D. J. Thompson, 1999, Journal of Sound and Vibration 226(2), 305–328. The use of an equivalent forces method for the experimental quantification of structural sound transmission in ships.
2. J. W. Verheij, 1997, International Journal of Acoustics and Vibration 2(1), 11–20. Inverse and reciprocity methods for machinery noise source characterization and sound path quantification Part 1: Sources.
3. J. W. Verheij, 1997, International Journal of Acoustics and Vibration 2(3), 103–112. Inverse and reciprocity methods for machinery noise source characterization and sound path quantification Part 2: Transmission paths.
4. A. N. Thite, and D. J. Thompson, 2000, ISVR Technical Memorandum No. 851. Study of indirect force determination and transfer path analysis using numerical simulations for a flat plate.
5. P. A. Nelson, and S. H. Yoon, 2000, Journal of Sound and Vibration 233(4), 643–668. Estimation of acoustic source strength by inverse methods: Part I, Conditioning of the inverse problem.
6. S. H. Yoon, and P. A. Nelson, 2000, Journal of Sound and Vibration 233(4), 669–705. Estimation of acoustic source strength by inverse methods: Part II, Experimental investigation of methods for choosing regularization parameters.
7. A. N. Thite, 2002, University of Southampton PhD Thesis. Inverse determination of structure-borne sound sources.
8. M. Allen, 1974, Technometrics 16, 125–127. The relationship between variable selection and data augmentation and a method for prediction.
9. G. H. Golub, M. Heath, and G. Wahba, 1979, Technometrics 21(2), 215–223. Generalized cross-validation as a method for choosing a good ridge parameter.

APPENDIX A

DERIVATION OF ORDINARY CROSS VALIDATION [6]

The ordinary cross validation function is defined by

$$V_O(\lambda) = \frac{1}{m}\sum_{k=1}^{m}\left|\hat{a}_k - \hat{A}_k\tilde{F}_k\right|^2 \tag{6}$$

where m is the number of responses, $\hat{a}_k$ is the kth measured operational response, and $\hat{A}_k\tilde{F}_k$ is the reconstructed response by the force vector obtained from the responses except the kth one, where $\hat{A}_k$ is a vector containing one row of $\hat{A}$.

The force vector $\tilde{F}_k$ is given by

$$\tilde{F}_k = (\hat{A}^H\hat{A} + \lambda I)^{-1}\hat{A}^H\hat{a}(k) \tag{A1}$$

where $\hat{a}(k) = [\hat{a}_1\ \hat{a}_2 \cdots \hat{a}_{k-1}\ a_k(\lambda,k)\ \hat{a}_{k+1} \cdots \hat{a}_m]^T$. Thus, the vector of estimated responses can be written as

$$a(\lambda,k) = \hat{A}\tilde{F}_k = \hat{A}(\hat{A}^H\hat{A} + \lambda I)^{-1}\hat{A}^H\hat{a}(k) = C(\lambda)\hat{a}(k) \tag{A2}$$

where the matrix $C(\lambda)$ is given by $\hat{A}(\hat{A}^H\hat{A} + \lambda I)^{-1}\hat{A}^H$. This relationship can be written in full as

$$\begin{bmatrix} a_1(\lambda,k) \\ a_2(\lambda,k) \\ \vdots \\ a_k(\lambda,k) \\ \vdots \\ a_m(\lambda,k) \end{bmatrix} = \begin{bmatrix} c_{11} & c_{12} & \cdots & c_{1m} \\ c_{21} & c_{22} & \cdots & c_{2m} \\ \vdots & \vdots & & \vdots \\ c_{k1} & c_{k2} & \cdots & c_{km} \\ \vdots & \vdots & & \vdots \\ c_{m1} & c_{m2} & \cdots & c_{mm} \end{bmatrix} \begin{bmatrix} \hat{a}_1 \\ \hat{a}_2 \\ \vdots \\ a_k(\lambda,k) \\ \vdots \\ \hat{a}_m \end{bmatrix} \tag{A3}$$

where c_{ij} are the components of matrix $C(\lambda)$. Now, the estimated responses using all measured responses can be written as

$$a(\lambda) = \hat{A}(\hat{A}^H\hat{A} + \lambda I)^{-1}\hat{A}^H\hat{a} = C(\lambda)\hat{a} \tag{A4}$$

and written again in full as

$$\begin{bmatrix} a_1(\lambda) \\ a_2(\lambda) \\ \vdots \\ a_k(\lambda) \\ \vdots \\ a_m(\lambda) \end{bmatrix} = \begin{bmatrix} c_{11} & c_{12} & \cdots & c_{1m} \\ c_{21} & c_{22} & \cdots & c_{2m} \\ \vdots & \vdots & & \vdots \\ c_{k1} & c_{k2} & \cdots & c_{km} \\ \vdots & \vdots & & \vdots \\ c_{m1} & c_{m2} & \cdots & c_{mm} \end{bmatrix} \begin{bmatrix} \hat{a}_1 \\ \hat{a}_2 \\ \vdots \\ \hat{a}_k \\ \vdots \\ \hat{a}_m \end{bmatrix}. \tag{A5}$$

From the above two matrix equations, a relationship between $a_k(\lambda,k)$ and $a_k(\lambda)$ can be derived. Therefore

$$a_k(\lambda,k) = c_{k1}\hat{a}_1 + c_{k2}\hat{a}_2 + \cdots + c_{kk}a_k(\lambda,k) + \cdots + c_{km}\hat{a}_m \tag{A6}$$

and

$$a_k(\lambda) = c_{k1}\hat{a}_1 + c_{k2}\hat{a}_2 + \cdots + c_{kk}\hat{a}_k + \cdots + c_{km}\hat{a}_m . \tag{A7}$$

The difference between these two equations shows that

$$(1 - c_{kk})a_k(\lambda,k) = a_k(\lambda) - c_{kk}\hat{a}_k . \tag{A8}$$

Therefore,

$$\hat{a}_k - a_k(\lambda,k) = \frac{\hat{a}_k - a_k(\lambda)}{1 - c_{kk}} . \tag{A9}$$

This enables the expression for the ordinary cross validation function $V_O(\lambda)$ given by equation (6) to be written as

$$V_O(\lambda) = \frac{1}{m}\sum_{k=1}^{m}\left[\frac{\hat{a}_k - a_k(\lambda)}{1 - c_{kk}}\right]^2 . \tag{A10}$$

Since $a(\lambda) = \hat{A}\tilde{F}(\lambda) = C(\lambda)\hat{a}$, this expression can be written as

$$V_O(\lambda) = \frac{1}{m}\left\|B(\lambda)(I - C(\lambda))\hat{a}\right\|^2 \tag{7}$$

where $\|\cdot\|$ indicates the Euclidean norm and $B(\lambda)$ is the diagonal matrix whose entries are given by $1/(1 - c_{kk}(\lambda))$.

APPENDIX B

CIRCULANT MATRICES

An $n \times n$ matrix, whose rows are composed of a cyclically shifted version of a length-n list $\{c_0, c_1, c_2, \cdots, c_{n-1}\}$, is called a circulant matrix and has the form

$$A = \begin{bmatrix} c_0 & c_{n-1} & c_{n-2} & \cdots & c_1 \\ c_1 & c_0 & c_{n-1} & \cdots & c_2 \\ c_2 & c_1 & c_0 & \cdots & c_3 \\ \vdots & \vdots & \vdots & & \vdots \\ c_{n-1} & c_{n-2} & c_{n-3} & \cdots & c_0 \end{bmatrix}. \tag{B1}$$

APPENDIX C

DERIVATION OF GENERALIZED CROSS VALIDATION

If the transformed model is given by

$$\tilde{e}_t = \hat{a}_t - \hat{A}_t \tilde{F}\,, \tag{15}$$

where $\tilde{e}_t = WU^H \tilde{e}$, $\hat{a}_t = WU^H \hat{a}$, and $\hat{A}_t = WSV^H$, and ordinary cross validation (7) is applied to this transformed model, then the generalized cross validation can be defined as

$$V_G(\lambda) = \frac{1}{m}\left\| B_t(\lambda)\left(I - C_t(\lambda)\right)\hat{a}_t \right\|^2, \tag{C1}$$

where $C_t(\lambda) = \hat{A}_t(\hat{A}_t^H \hat{A}_t + \lambda I)^{-1}\hat{A}_t^H$ and $B_t(\lambda)$ is the diagonal matrix whose entries are given by $1/\left(1 - c_{t,kk}(\lambda)\right)$, $c_{t,kk}(\lambda)$ being the kkth entry of $C_t(\lambda)$ and constant because $C_t(\lambda)$ is a circulant matrix (see Appendix B). Therefore

$$B_t(\lambda) = \frac{1}{1 - c_{t,11}(\lambda)} I_B = \frac{1}{(1/m)Tr(I - C_t(\lambda))} I_B \tag{C2}$$

where I_B is the identity matrix with same size to $B_t(\lambda)$. Substituting equation (C2) into equation (C1), the generalized cross validation function can be written as

$$V_G(\lambda) = \frac{(1/m)\left\|(I - C_t(\lambda))\hat{a}_t\right\|^2}{[(1/m)\mathrm{Tr}(I - C_t(\lambda))]^2}. \tag{16}$$

where $C_t(\lambda)$ is a circulant matrix and thus constant along the diagonals.

Since $C(\lambda)$ and $C_t(\lambda)$ have the same eigenvalues as below

$$C(\lambda) = \hat{A}\left(\hat{A}^H\hat{A} + \lambda I\right)^{-1}\hat{A}^H = US\left(S^H S + \lambda I\right)^{-1} S^H U^H = U\Lambda U^H, \tag{C3}$$

and

$$C_t(\lambda) = \hat{A}_t\left(\hat{A}_t^H\hat{A}_t + \lambda I\right)^{-1}\hat{A}_t^H = WS\left(S^H S + \lambda I\right)^{-1} S^H W^H = W\Lambda W^H, \tag{C4}$$

where $\Lambda = S\left(S^H S + \lambda I\right)^{-1} S^H$ is the diagonal matrix with eigenvalues, hence the traces of $C(\lambda)$ and $C_t(\lambda)$ are equal to each other,

$$\mathrm{Tr}\left(C(\lambda)\right) = \mathrm{Tr}\left(C_t(\lambda)\right), \tag{C5}$$

and the norm of the numerator of equation (16) is

$$\begin{aligned} \left\|\left(I - C_t(\lambda)\right)\hat{a}_t\right\| &= \left\|\left(I - W\Lambda W^H\right)WU^H\hat{a}\right\| = \left\|W\left(I - \Lambda\right)U^H\hat{a}\right\| \\ &= \left\|WU^H\left(I - U\Lambda U^H\right)\hat{a}\right\| = \left\|WU^H\left(I - C(\lambda)\right)\hat{a}\right\| \\ &= \left\|\left(I - C(\lambda)\right)\hat{a}\right\| \end{aligned} \tag{C6}$$

because W and U^H are unitary matrices.

Therefore, equation (16) can be written as

$$V_G(\lambda) = \frac{(1/m)\left\|(I - C(\lambda))\hat{a}\right\|^2}{[(1/m)\mathrm{Tr}(I - C(\lambda))]^2}. \tag{17}$$